Evaluation of the handling of a variable dynamics tilting tricycle:

A novel handling evaluation method

Floris van Willigen

June 2023
TU Delft

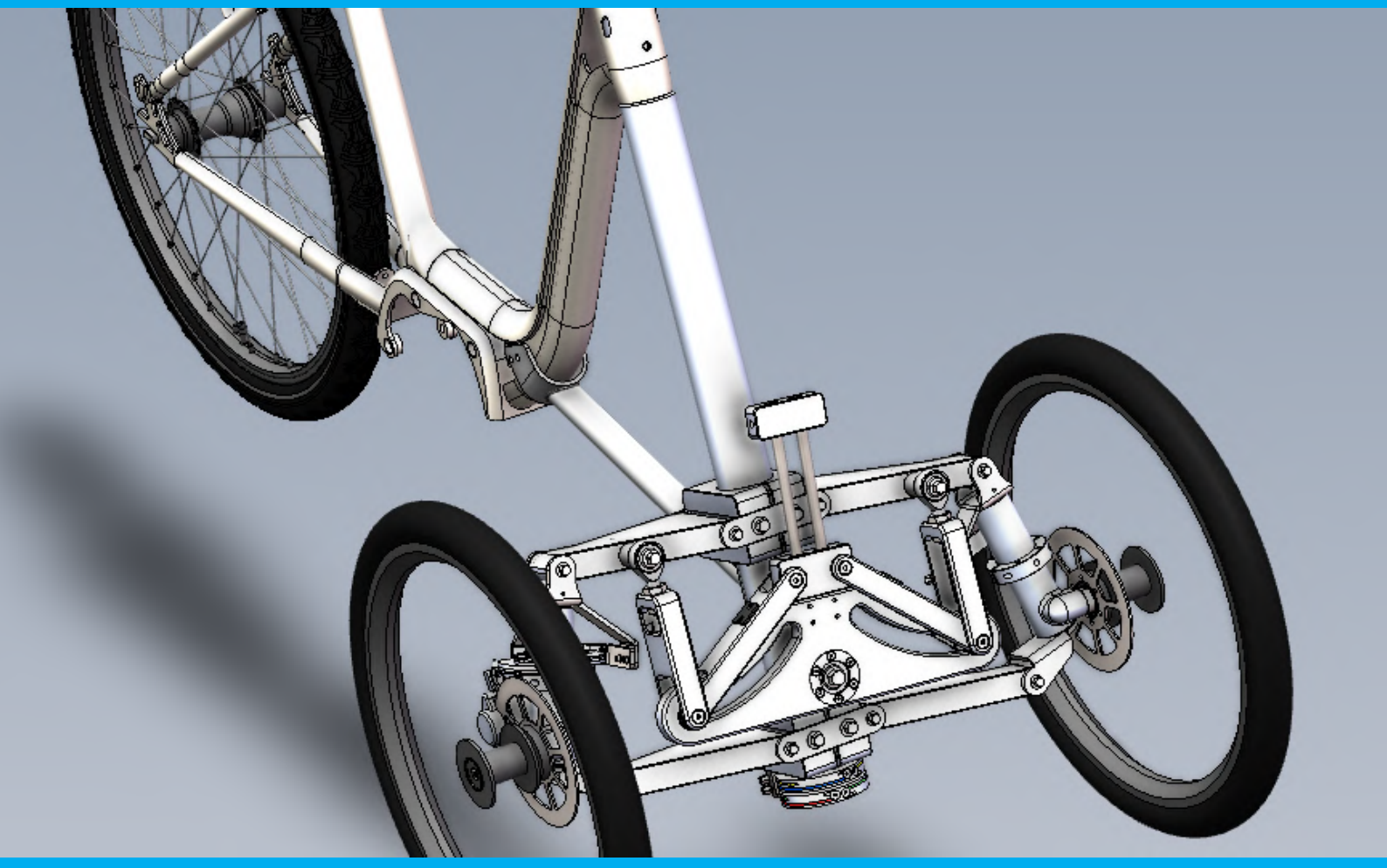

TU Delft

Evaluation of the handling of a variable dynamics tilting tricycle

A novel handling quality evaluation method

by

Floris van Willigen

Floris	van Willigen
Student number	4694228

Supervisor:	J.K. Moore
Daily Supervisor:	A. Dressel
Project Duration:	November, 2022 - June, 2023
Faculty:	Faculty of Mechanical, Maritime and Materials Engineering (3Me), Delft

TU Delft

Preface

My interest in dynamics, sensors, and mechanical optimization has led me to the subject of the thesis that lies before you. The thesis ”Evaluation of the handling of a variable dynamics tilting tricycle” has been written to fulfill the graduation requirements of a master’s degree in Mechanical Engineering. This study has been fulfilled between November 2022 and June 2023.

This study has shown me how interesting it can be to start extensive research and dive deep. After more than 200 trials and months of hard work, this thesis has taught me that being stuck at some point only shows that you are on the way to learning new things. It has engaged me to try the vehicles of the future during this research and being able to collaborate on new developments that can potentially make city traffic safer, more sustainable, and more comfortable, brings me joy.

I want to thank my daily supervisor, Andrew Dressel, that has been there for good discussions about the progress and the motivating meetings. I want to thank my supervisor Jason Moore for the excellent guidance through the process of graduation. I also want to thank Piet Noordzij for letting me test his tricycles during the study and the developers at DEMO for the hard work that delivered the Dressel tricycle. Furthermore, I want to thank all bicycle lab members for the good fun and my family and friends for their support.

Finally, I also want to thank you, my reader, I hope you enjoy reading this thesis report.

Floris van Willigen
Delft, June 2023

Abstract

The favorite way of transport for commuters is still by cars, which are designed too heavy and too wide for the average amount of passengers. Accidents without other traffic users make up a large proportion of crashes for free-tilting bicycles. Tricycles have a chance of rollover while cornering fast. Therefore, new human-powered commuter vehicles are needed that have optimized handling performance and are safer.

This alternative can be the narrow tilting tricycle, with the combined advantages of bicycles and tricycles. Faster cornering can be performed than with a tricycle, and better balance and more traction can be obtained than with a bicycle.

No method exists to evaluate the handling performance of a narrow tilting tricycle that gives a combined conclusion about the handling performance for multiple velocities and aspects of handling. This study evaluated the optimized handling performance for commuting for a prototype tilting tricycle. The tricycle is designed by Andrew Dressel and built by DEMO at TU Delft. The tilt mechanism incorporates tie rods that connect A-arms to the bell crank at adjustable connection points. This coordinates the tilt behaviour which changes with different connections from the tie rods to the bell crank.

I created a novel handling evaluation method for commuter vehicles in a quantitative within-subjects study. I selected a moderate-speed slalom manoeuvre and a low-speed line-following manoeuvre as test manoeuvres. I have measured the maximum yaw factor, the mean absolute steer angle, and the time delay between the roll rate and steer as handling metrics using two Shimmer3 IMUs. The first metric is evaluated for the slalom manoeuvre and the second and third metrics are evaluated for the low-speed line-following manoeuvre. I scaled the metrics and combined the results into a single score.

The selected metrics are able to discriminate between the performance of conventional bicycles and prototypes of tilting tricycles. For highly similar designs, it is important to add trials until statistical significance can be reached.

The analysis of the data showed the optimal handling performance of the Dressel tilting tricycle for tie rod angles halfway between free-tilting and self-stable when stationary. For commuter vehicles in city traffic, the tie rods can be fixed at 50%. Increased low-speed balance is proven for increased tie rod angles, without finding reduced performance on the moderate-speed slalom. It is not recommended to increase the tie rod angle to 75%. Uncontrollable performance has been observed in this configuration. A tie rod angle of 100% can provide complete rigidity while standing still.

The tilt limit has been hit with increased tie rod angles and this limit is increased with a Matlab optimization. For the optimal configuration with tie rods connected halfway in, the bell crank should be designed 380 mm wide and connected 235 mm high from the ground.

The tilt mechanism with the optimal design parameters can make the vehicle safer because of the improved balance, without reducing the handling performance. A fixed design can make the vehicle cheaper and easier to build compared to the adaptable tilting tricycle.

Contents

List of Figures

List of Abbreviations

Abbreviation	Definition
BCO	Bell Crank Offset
BCW	Bell Crank Width
DEMO	Dienst Elektronische en Mechanische Ontwikkeling
ER	Emergency Room
HQM	Handling Quality Metric
IMU	Initial Measurement Unit
PLA	PolyLactic Acid
SD	Standard Deviation
TRA	Tie Rod Angle

1

Chapter 1: Introduction

1.1. Tilting tricycles

The world is shifting towards more sustainable forms of transport to keep the climate stable and to reach the climate agreement of Paris in 2016. However, since the beginning of the industrial age in 1970, the global carbon dioxide (CO_2) emission of the transport sector has been rising, as shown in figure 1.1 [38]. The only exception to this is the COVID-19 pandemic. Present day, the CO_2 emission of the transport sector accounts for roughly 22% of the annual worldwide emission of greenhouse gasses, of which the emission leads to global warming [2].

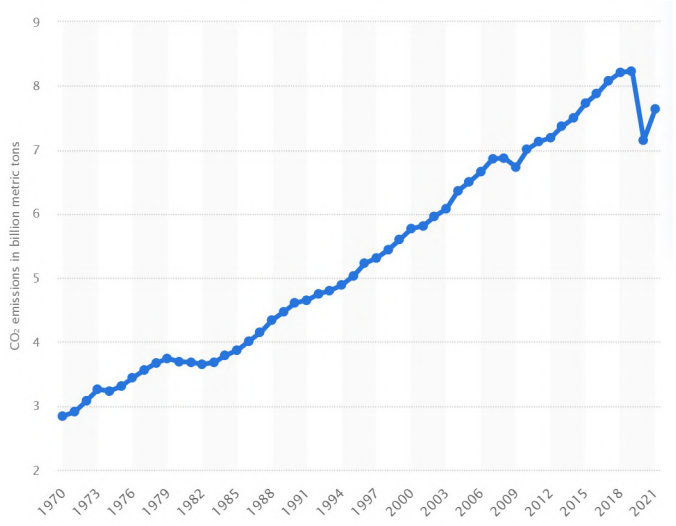

Figure 1.1: The worldwide CO_2 emissions of the transport sector between 1970 and 2021 [38].

Seventy-seven percent of the trips by car in the United States (U.S.) are shorter than 16 kilometers. This short range offers opportunities for more sustainable human-powered vehicles [30]. However, figure 1.2 shows that the largest group of commuters in the U.S. still choose cars over bicycles and motorcycles [24].

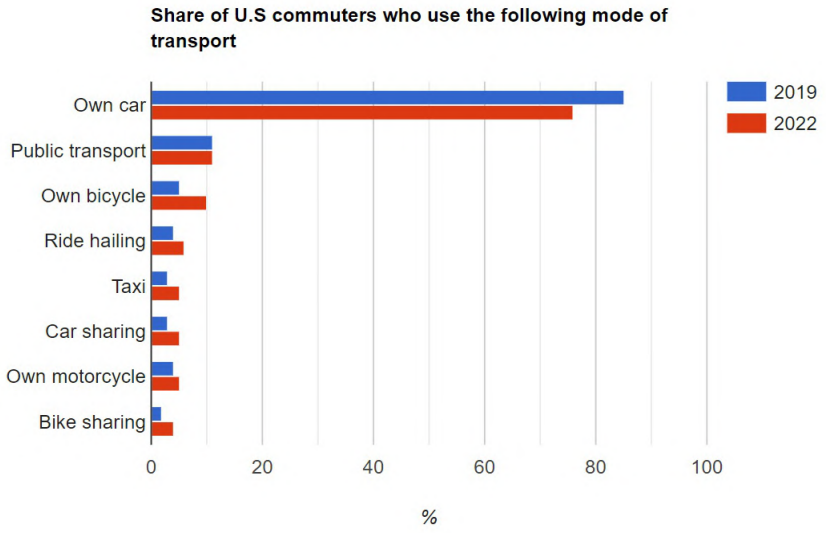

Figure 1.2: The share of U.S citizens that choose the following vehicles for commuting [24].

Furthermore, the average number of passengers transported by a car is only 1.58 people, and therefore the vehicles are typically too wide and too heavy [7]. This means as well that cars take more pavement than necessary, leading to more traffic jams.

If more people would shift from taking a car to a sustainable, human-powered vehicle for a single person, this would decrease the emission of greenhouse gasses. In economic terms, human-powered commuter vehicles are also cheaper for the customer and quicker to manufacture.

The current options for human-powered commuter vehicles include upright and recumbent bicycles and tricycles, possibly supported by electrical assistance. These options can be made safer and more comfortable, to persuade more users for commuting using other alternative ways of transport. In terms of safety, many casualties occur using bicycles. In the Netherlands, a paramount country in the use of bicycles, the number of accidents where no other vehicle has been involved (single-sided accidents), has led to 48000 cases at the emergency room (ER) in a single year [39]. These single-sided accidents accounted for two-thirds of the total cases of bicycle accidents that ended up in hospitals [39].

The narrow tilting vehicle represents an innovative solution that can provide safer and more comfortable transportation for commuting and leisure. These vehicles utilize three wheels to leverage the benefits of a tricycle. The benefits can include increased stability, improved traction on the road, and potentially enhanced acceleration and braking performance.

The vehicles incorporate a tilt mechanism, which allows them to use these advantages without the downsides of a tricycle. The main downside is the chance of rolling over while cornering at high speed. The mechanism allows them to tilt like a bicycle, so the vehicle can go just as fast through corners as a bicycle, and the chance of rolling over is reduced. This can also lead to more comfortable riding on uneven terrains than with regular tricycles as the wheels adapt to the angle of the road.

The tilt mechanism is a key feature of tilting tricycles, which allows riders to lean into turns while maintaining stability and control. These tilt mechanisms are comprised of three main categories, the parallelogram, the bell crank with swing arms, and the crank mechanism [32]. Figure 1.3 shows the three categories of the tilt mechanisms.

Figure 1.3: The three main categories of tilt mechanisms. From left to right: The parallelogram, the bell crank plus swing arm design, and the crank mechanism [32].

The bell crank plus swing arm mechanism uses a bell crank and swing arm to connect the steering and tilting mechanisms. The middle image of figure 1.3 shows the rotating bell crank that facilitates the tilt, usually placed at the symmetry plane of the tricycle. The swing arms connect the wheels to the central part of the mechanism. This mechanism can be used for tricycles with two rear wheels, the delta design. The crank mechanism employs pedal cranks at the connection of the two wheels to the frame, to make sure the vehicle can tilt, as can be seen in the right image of figure 1.3. This mechanism can be realized for tricycles in the delta design. The parallelogram mechanism uses a four-bar linkage to connect the steering and tilting mechanisms, which is easier to design for tricycles with two front wheels, the tadpole design. A parallelogram can be recognized in the bar linkage of the tilt mechanism in the left image of figure 1.3.

The mechanism choice mostly matters for manufacturing. The best mechanism depends on the design of the tricycle and the mechanism needs to be combined with a steering system for convenient usage of the vehicle.

A tilting tricycle with an adjustable tilt mechanism has been designed by Dressel and manufactured by Dienst Elektronische en Mechanische Ontwikkeling (DEMO) at TU Delft. This thesis focuses on the optimal design of a custom tilt mechanism of the Dressel tilting tricycle for optimal handling.

This vehicle has a unique design of the tilt mechanism that makes use of parts that combine the parallelogram and the bell crank mechanisms, with variable settings. The working and details of the mechanism will be explained in chapter 5. The SolidWorks model of the tricycle is shown in figure 1.4.

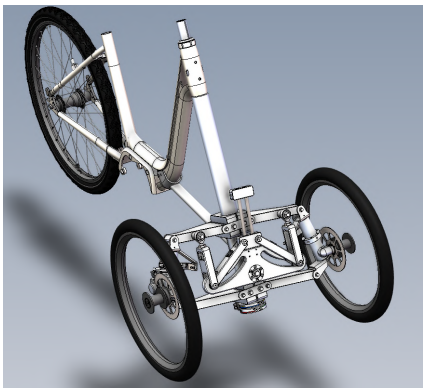

Figure 1.4: The complete design of the tilting tricycle.

Changing the setting of the adjustable tilt mechanism alters the kinematics of the vehicle. This leads to custom behaviour ranging from free-tilting like a bicycle, to fully rigid like a tricycle, with settings in between. The settings in between make the trajectory of the roll of the tricycle follow the path of a taller bicycle, which slows down the roll. This will also be explained in more detail in chapter 5.

It is hypothesized that a specific design of the tilt mechanism will lead to optimal handling performance. No study has yet been performed that optimizes the tilt mechanism of a tilting tricycle for optimal handling performance.

1.2. Handling evaluation

Although significant research has been conducted on the dynamics of bicycles and motorcycles, there is a paucity of quantitative research on the handling performance of tilting tricycles and their comparison to conventional bicycles. Also, the handling tests in the literature focus on single tests for a single velocity, rather than investigating the handling performance of a vehicle in the broadest sense for a larger operating range.

To address this gap, this thesis introduces a novel handling quality assessment method specifically designed for commuter vehicles. This method combines important factors that affect handling performance in both low-speed and moderate-speed velocity regions, where most commuter vehicles operate. With this method, the performance of different vehicles and configurations can be analyzed and compared, leading to the selection of the optimal tilt mechanism configuration for the Dressel tilting tricycle. This offers valuable insights into the handling performance of tilting tricycles and their potential as a safer and more sustainable transportation option for commuters in city traffic.

1.3. Research approach

The aim of this thesis is to optimize the geometrical parameters of the tilt mechanism of the tilting tricycle for optimal handling for commuting. This means that handling performance for racing will not be investigated and everyday city traffic is the main aim of this research. An experimental study will be conducted to answer the following research question:

How can the tilt mechanism of the narrow tilting tricycle be designed for optimal handling performance for commuter vehicles?

To reach this goal, the thesis is built up from multiple steps and subquestions that need to be answered to have a clear view of the results.

- What is the best method to evaluate handling for commuter vehicles?
- How well can the method discriminate handling performance between vehicles?
- In which configuration is the handling performance optimal?
- Can the vehicle be made safer by optimizing the tilt limit?

In total, this will lead to the answer to the research question.

1.4. Thesis outline

To answer the research question and the described subquestions, chapter 2 will investigate the most appropriate way to evaluate the handling performance for commuting. Metrics will be selected that can be measured during physical handling tests. After this, experiments will be performed with three types of vehicles. Chapter 2 contains the protocol of the experiments. The results of the first experiments are described in chapter 3. This experiment sets a reference score that will be used for the normalization scale and evaluates how well the combined handling score can distinguish between a change in the design of free-tilting bicycles. The second experiment, described in chapter 4, will test two tilting tricycles with a fixed geometry, which can be used to conclude the suitability of the method for tilting tricycles. The third experiment, described in chapter 5, will test the adaptable geometry of the Dressel vehicle in multiple configurations, to evaluate at which configuration the handling performance is optimal. The optimal parameters of the geometry of the mechanism can now be selected. After this has been completed, chapter 6 will explore whether the vehicle's safety can be improved by increasing the tilt limits, by using a Matlab optimization.

2

Chapter 2: Handling quality evaluation

Handling is a term that refers to how well a vehicle responds to the driver's input and how easily it can be maneuvered. Good handling is characterized by a vehicle that is stable, predictable, and responsive, allowing the driver to control it smoothly and safely [21].

To determine the most suitable method for measuring handling performance in commuter vehicles under city traffic conditions, this section provides essential background information. The chosen method serves as the base for concluding the handling performance. Moreover, the method is developed to be able to differentiate the handling performance of different vehicles.

2.1. Handling metrics background

This section contains information about how physical parameters affect handling. It addresses information from the literature. Furthermore, the methods to quantify and measure handling performance are investigated.

2.1.1. Design for handling

In bicycle design, parameters such as the trail, head angle, wheelbase, weight, tire width, and mass moments of inertia can all lead to different perceived handling [31]. Bicycle designers keep these parameters in mind when aiming for a specific use for the bicycle.

This thesis develops a method to evaluate the handling performance of single and narrow-track vehicles. It is valuable to be able to interpret the results in terms of known relations between design parameters and handling.

The described measures of the trail, head angle, wheelbase, and rake are defined according to figure 2.1.

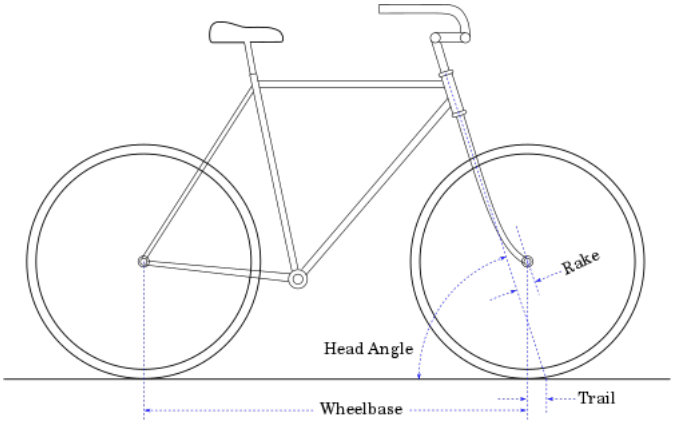

Figure 2.1: The important dimensions of the bicycle that are used in this thesis [4].

Few studies investigate the effect of design parameters on handling qualities. However, Paterek (2004) describes in his manual for frame builders that the comfort range for the trail of the bicycle is between 50 and 65 mm [31]. Moore (2006) shows that the low-speed stability increases for a decreased trail, decreased wheelbase, and a medium head angle [26]. There is no study that investigates the effect of the frame properties on the handling qualities at higher speeds.

This information can partly be used as a base to interpret the handling performance obtained in this thesis while comparing vehicles.

2.1.2. Handling quality evaluation methods

The measurement of handling quality has its origins in the aircraft industry, where it was initially evaluated using a subjective scale called the Cooper-Harper scale [21]. Nowadays, handling is often assessed using both objective and subjective scales. Subjective handling evaluation assesses the rider's perception of the handling performance, while objective evaluation quantifies the handling performance using specific metrics. To specifically investigate the objective measures of handling, some researchers, such as Cossalter (1999), use the term maneuverability to indicate the quality and agility of a vehicle's maneuvers [9]. This thesis focuses on analyzing the objective measures of handling, rather than the subjective ones.

Various efforts have been made in previous research to measure the handling performance of bicycles and motorcycles. I reviewed the literature to identify the most suitable handling metrics and the most suitable tests have been designed.

The Handling Quality Metric (HQM) is a metric that originates from airplane-pilot control theory. The metric has been used by researchers to model bicycles for optimal handling using a theoretical rider model and the Whipple-Carvalho bicycle model [27, 28]. The HQM is also applied to optimize handling performance for bicycles. In this case, the HQM uses the magnitude of the effort of the rider to investigate the handling. The authors state that the handling qualities of bicycles can be reflected in the magnitude of the closed loop transfer function between the commanded input (C) and the primary rate loop variable (U_M), normalized by the gain K_p [27]:

$$HQM = \left| \frac{U_M}{C}(jw) \right| \frac{1}{K_p} \tag{2.1}$$

The transfer function can conclude how well a rider can track the roll rate of the vehicle. For some parts of this study, vehicles are compared that have roll resistance. Because these vehicles can keep themselves upright better than bicycles, the HQM is not suitable to test the handling performance of all vehicles in this study.

This study investigates a method where other simple handling tests can conclude on the quantitative handling performance of different kinds of vehicles in practice. Multiple other handling tests have been

developed in past research with respective handling metrics that can measure aspects of handling performance.

According to Rice et al., (1978), Zellner and Weir (1979), Koch (1980), and Cossalter (2006), the handling performance of the vehicle can be calculated by the measurable relation between some input and output data on the vehicle, with a possible normalization [10, 19, 33, 42]. The Koch index (equation 2.2) and the similar and later derived LC index (equation 2.3) show to be valuable metrics to calculate the handling performance, but the input handlebar torque is a required measure [21]. The Koch index relates the peak torque to the peak roll rate during a U-turn manoeuvre[19]. The LC index is similar, although it relates the peak-to-peak torque input to the peak-to-peak roll rate during a lane change manoeuvre [10]. Both metrics are normalized with speed. In the equations, τ represents the handlebar torque, V represents the velocity of the vehicle and $\dot{\varphi}$ represents the roll rate of the vehicle.

$$\text{Koch index} = \frac{\tau_{peak}}{V\dot{\varphi}_{peak}} \tag{2.2}$$

$$\text{LC index} = \frac{\tau_{p-p}}{V_{avg}\dot{\varphi}_{p-p}} \tag{2.3}$$

During the literature review phase, I investigated methods to measure the handlebar torque for the handling tests in this study, but I decided that this can be too inaccurate, time-consuming, and costly for the scope of the research.

Other handling metrics make use of kinematic data only. Often, only one metric is calculated in one manoeuvre. In the context of commuting, the versatility of the vehicle necessitates the measurement of handling performance across multiple manoeuvers for different velocities. All single metrics that have been found in the literature give insight into a single aspect of handling performance. To obtain a single score for a broad aspect of handling performance, I combine metrics that evaluate handling performance at both low-speed and moderate-speed regions and manoeuvers in this thesis.

I choose to calculate the handling performance over three independent handling metrics that cover independent aspects of the handling performance of commuting vehicles to conclude the most on the general handling performance. The metrics and their characteristics are discussed in more detail in the next section.

These metrics have a specific test that is the most suitable for the metric. For each handling metric, I select the most suitable manoeuvre and design the most suitable test, based on the literature. In contrast to the car industry, there are no standardized handling manoeuvres for bicycles [15]. The total score of the handling index can be obtained by combining the scores from the metrics, which is explained in section 2.3.2.

2.2. Selected handling metrics

This section contains the selected handling metrics and explains why and how these metrics can be used to conclude the total handling performance of a commuter vehicle for city traffic.

2.2.1. Maximum Yaw factor

The first metric that has been selected is the maximum value of the yaw factor, defined as the yaw rate over the steer angle, $\frac{\dot{\psi}}{\delta}$.

This metric is a measure of the steer response of the vehicle, with the steer angle as input and the yaw rate as output [18, 21, 40, 41]. This means that an optimized score for the metric can lead to a controllable steer characteristic.

Zellner and Weir used it in 1978 in a quantitative study to test and compare the handling characteristic of motorcycles for low up to high velocities [41]. Klein and Hogue (1979) used the factor as a key handling factor to optimize their controller to control the steer responses with perturbation due to crosswind [18]. Yu et al., (2016) evaluated the metric during an obstacle avoidance manoeuvre, and they showed how the factor decreased for improved handling [40].

The yaw factor is determined at the least smooth part of the manoeuvre, this way the startup time and all parts of the manoeuvre where the vehicle does not undergo any problems in terms of manoeuvrability, are not investigated. This leads to a metric in the form of the maximum value of the yaw factor, that is able to show problems with the control of the steering. As the vehicle is obligated to complete the manoeuvre at a given speed, the steer response should stay controllable. The maximum yaw factor should therefore ideally be as low as possible [21, 41].

A high maximum yaw factor can show uncontrollable and too sharp steering when controllable steady turning is desired.

This metric is suitable to measure at moderate speeds of the commuter vehicle. The metric has been used to measure and optimize the performance of vehicles in previous studies, but it has never been used to compare the performance of human-powered vehicles. In this study, it has been investigated if it can distinguish between vehicles to compare the handling performance in a slalom.

A slalom manoeuvre has been selected as the most appropriate manoeuvre to evaluate this metric, and this manoeuvre captures the agile cornering motion that is desired for the good handling of a commuter vehicle. Cones have been used to create the slalom track. Section 2.4.2 shows the track in more detail. A good slalom has smooth turns closely around the cones. To have less variation in the maximum yaw factor during the manoeuvre, the rider ideally accelerates before the start of the cone trail and performs the manoeuvre with a velocity that is as constant as possible.

According to the linearized benchmark equations of motion, the yaw rate is defined as [36]:

$$\dot{\psi} = \frac{v\delta + c\dot{\delta}}{w} Cos(\lambda) \tag{2.4}$$

The yaw factor can thus be given as:

$$\frac{\dot{\psi}}{\delta} = (\frac{v}{w} + \frac{c\dot{\delta}}{w\delta}) Cos(\lambda) \tag{2.5}$$

In this equation, v represents the forward velocity of the vehicle, c represents the trail, w represents the wheelbase and λ represents the head angle. The steer angle and steer rate are defined by δ and $\dot{\delta}$, respectively.

It can be seen that there is a dependency on velocity that cannot be normalized. Because of that, the test has to be done at a constant speed to be able to compare the scores between similar vehicles. When a vehicle is only capable of performing the manoeuvre at a lower maximum speed than another vehicle, a correction can be made, $\frac{\dot{\psi}}{\delta}^*$. The difference in velocity can be added to have a theoretical comparison with the other vehicles on a higher velocity. It is investigated if this theoretical relation fits compared to the obtained data. A more in-depth analysis of this relation can be found in section 5.2.1.

2.2.2. Mean absolute steer angle

This metric is related to the low-speed balance of the vehicle. When the rider is riding the vehicle at low speed, the rider needs to apply input to keep the vehicle upright and the vehicle deviates from the intended path of the rider. It is hypothesized that if there is a better handling performance of the vehicle, the rider needs to correct the steering with less effort while trying to ride straight at low speeds. A larger absolute mean steer angle indicates that the fluctuations of the steering wheel are larger, suggesting more problems with balance and tracking the intended path. The low speed leads to shaky steering and this can be related to the handling performance. This metric is related to the low-speed balance of the vehicle. When the rider is riding the vehicle at low speed, the rider needs to apply input to keep the vehicle upright and the vehicle deviates from the intended path of the rider. It is hypothesized that if there is a better handling performance of the vehicle, the rider needs to correct the steering with less effort while trying to ride straight at low speeds. A larger absolute mean steer angle indicates that the fluctuations of the steering wheel are larger, suggesting more problems with balance and tracking the intended path. This metric is suitable to measure with a low-speed manoeuvre, as the corrections on the steering wheel are harder and shakier at slow velocities. This makes it easier to discriminate between

designs. Good conclusions related to the handling could be obtained from a study by Kovacsova et al., (2016). The authors used the metric to investigate the differences in performance between middle-aged and older riders and also for different vehicles [22].

The metric is calculated for straight riding along a line. The goal is to stay on the line perfectly. When the vehicle deviates because the path is harder to control due to the roll of the vehicle, the goal is to correct the vehicle back onto the line by steering. The track of the manoeuvre can be found in section 2.4.2.

It is important that the manoeuvre is performed with a constant speed, as maintaining a straight path becomes easier with higher speeds.

2.2.3. Average time delay between steer rate and roll rate

The steer rate and roll rate are highly correlated, at some time delay. This has been investigated in the late 20th century by Doyle (1987) and later by Cain et al., (2012,2016) [5, 6, 14]. A bicycle can keep itself upright by steering into the lean. When a bicycle does this on its own at the correct amount, it exhibits self-stability [20, 35].

The average time lag between steer rate and roll rate indicates the responsiveness of the vehicle to inputs of the rider and is dependent on the geometry, weight distribution, and speed. Typically, the steer rate lags behind the roll rate [5, 6, 14, 22].

In previous research that has a comparable nature, this metric has been shown to be able to discriminate the handling performance of a vehicle with different groups of riders, it has also been shown that it could discriminate between two types of vehicles for the same group of riders [22]. A low time delay indicates that quick response of the vehicle is present and that can lead to good manoeuvrability. This can make an impact when quick responses are required and that makes the vehicle safer as well, for instance when obstacles need to be avoided.

The time delay between the steer rate and roll rate can be calculated using the cross-correlation between the signals. The peak in the cross-correlation chart shows at what time shift, the signals have the highest similarity. This is the average time delay between the signals. An example of this can be seen in figure 2.2. The normalized cross-correlation has been plotted of a sampled arbitrary vector compared to the same vector that is shifted by five samples.

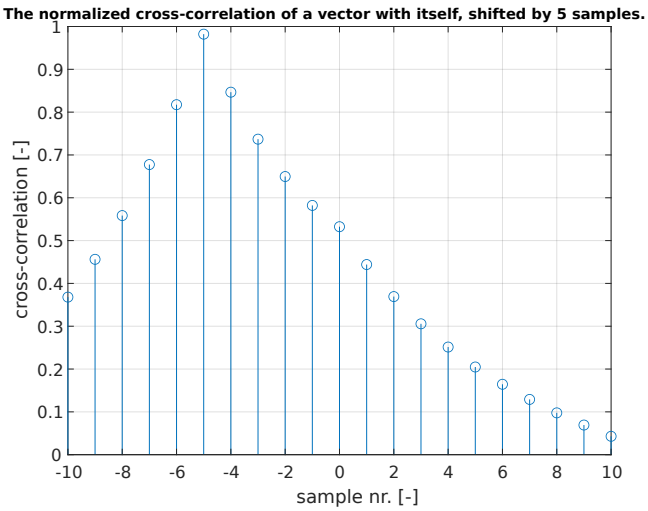

Figure 2.2: The normalized cross-correlation for a sampled arbitrary vector with itself, but shifted by five samples.

This metric is suitable to measure in slow manoeuvres as well, as the correlation and the time delay are less present at higher speeds and captures the capability of the vehicle to handle well in slow-riding situations that can occur in city traffic [5, 6].

To save time in the trials, this metric can be calculated in the same manoeuvre as the mean absolute steer angle. Section 2.4 describes the protocol of the experiments that are performed that make use of these three metrics to finally be able to answer the research question. The requirements for the measurement equipment that is minimally needed to measure the required kinematic states of the vehicle can be found in section 2.4.1.

2.3. Scoring

The scores of the metrics are scaled and combined into the combined handling score. This is explained in this section.

2.3.1. Scaling

Scale factors have been added that have the possibility to change the importance of each metric. However, in this study, the scale factors are only used to ensure the same order of magnitude for each metric. The scale factors are $\alpha_1, \alpha_2, \alpha_3$. The score of the metrics are M_1, M_2, M_3. To make sure that the three metrics have the same order of magnitude, $\alpha_1 = 10$, $\alpha_2 = 10$, and $\alpha_3 = 0.2$. These numbers have been determined using the mean performance of the reference bicycle, which will be introduced in the next chapter. A new user of this method can change the scale factors if the functionality of the vehicle is focused more on the high speed than the low speed of the commuter vehicle, or vice versa.

2.3.2. Combination

Together, these three metrics give a broad view of the total handling performance for commuting. The metrics that are described in the previous paragraph need to be combined into a single score to compare the handling performance between designs. For all metrics, a lower number indicates a better performance. Therefore, the reciprocals of the outcomes of the metrics need to be used before the scores can be added.

The metrics are added with a logarithmic scale, such that a good score is obtained when each of the metrics leads to a good score in total. If one of the three metrics has a worse score, the total score is affected quickly. This logarithmic function is concave ($\cap$), which has the right behaviour when one metric is low. Equation 2.6 shows the function that is used to calculate the combined handling score.

$$Score = log(\alpha_1 M_1) + log(\alpha_2 M_2) + log(\alpha_3 M_3) \tag{2.6}$$

Linear addition and nonlinear addition by the use of the magnitude of the vector have not been selected. The convex behaviour of this grading curve is not as desired. A convex function ($\cup$) is not suitable when one of the metrics is low.

For a two-metric situation, the logarithmic function is visualized in figure 2.3a and 2.3b. The two other combination methods are also plotted to be able to compare the more appropriate convex shape of the selected method with the less appropriate shapes. In green, the selected log scale can be seen. In blue, the magnitude of the vector is plotted, and in red, the linear scale is visualized. The desired shape of the logarithmic function can be seen. In reality, a three-metric situation occurs, which would require four dimensions to visualize.

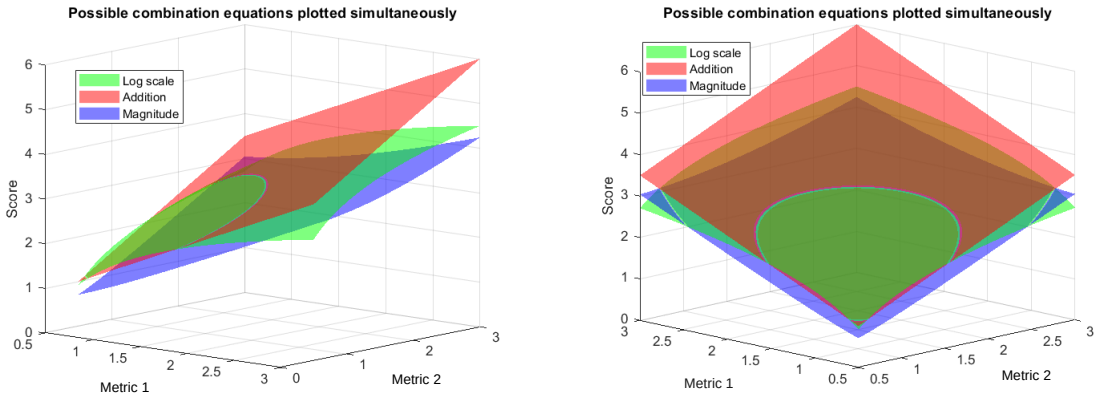

(a) Side-view. **(b)** Front-view.

Figure 2.3: The three possible methods of combining the three metrics. In green, is the log scale, in red, is the addition of the metrics, and in blue, is the magnitude of the vector of the metrics.

After the scores of the metrics are combined, the combined score is normalized in a range from [0,1]. The bounds of this normalization are discussed in the first experiment, in chapter 3. This is done only for visualization purposes along the normalized scale.

2.4. Experimental methods

This section contains the general experimental methods and the protocol for the handling tests that are performed in this study. The methods that are found here apply to all different vehicle types, which are explained in later chapters.

It is desired to keep as many factors as possible of the rider constant, so one participant will perform the test for multiple trials in a repeated measures within-subject experiment. This way, the participant's posture, the body's motion, and the rider's skill level are more constant over the trials than would be with multiple different participants. Furthermore, more trials can be collected with this type of study. The participant is a 23-year-old male with a height of 188 cm and a mass of 88 kg. This study does not include measurements of the motion of the body of the rider during the tests.

2.4.1. Equipment

To be able to calculate the selected handling metrics, kinematic data needs to be collected with the use of sensors.

Angular rates

It became clear from section 2.2 that the required signals are the vehicle's yaw rate, roll rate, and steer rate. The yaw rate and the roll rate correspond to the rate of change in the orientation of the frame of the vehicle. The steer rate is the difference between the yaw rate of the frame of the vehicle and the yaw rate of the front wheel. The following minimal requirements are set up for the instrumentation:

- The sampling frequency minimally needs to be 50 Hz, as Kovacsova et al., (2016) were able to draw good conclusions for similar tests with this sampling frequency [22].
- The sensors need to be switchable between vehicles relatively quickly, as many vehicles have to be measured at different locations in this study.
- A range larger than 200 degrees per second is needed to capture all angular velocities, this has been sufficient for typical data obtained by Kovacsova et al., (2016) [22].

The angular rates are measured using the gyroscope of two Shimmer3 Initial Measurement Units (IMUs). The accelerometer and magnetometer that are also built-in into the IMUs are not used in this study. These sensors fulfill the minimal requirements. The sampling frequency can be selected up to a maximum of 2048 Hz. These canned IMUs of only 51 x 34 x 14 mm are easy to switch between vehicles. The range of the IMU can be set up to 2000 degrees per second, but a range of 250 degrees

per second is used for higher sensitivity. This range suffices. The resolution of the gyroscope is 16-bit. These specifications are based on the manufacturer's datasheet [12].

One IMU is connected to the rear frame of the vehicle. When the rear frame of the vehicle is not suitable for attachment, the sensor is attached to the cargo rack. Because angular rates are measured, the resulting data is not dependent on the height or lateral connection point of the sensor. The other IMU is connected to the handlebars. This way, the signals can be recorded.

To connect the sensors, the IMUs are held by GUB Pro2 phone mounts. To fix the connection between the IMU and the phone mount, custom clips have been 3D printed using PolyLactic Acid (PLA) with an infill of 100%, figure 2.4a. The size of the clips allows for tight holding by the phone mount, and the sensors are clicked in using the slots on the side of the sensors. There are slits available in the clips, that can be used if one of the IMUs needs to be connected to the cargo rack. The Shimmer IMU can be seen while being held by the clip and the mount in figure 2.4b.

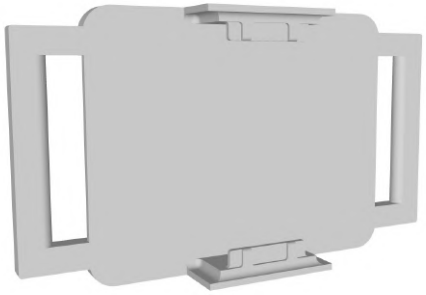

(a) The STL file of the 3D printed clamp for the Shimmer IMU.

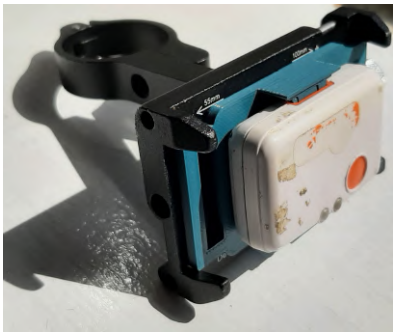

(b) The GUB Pro2 phone mount with the 3D printed clamp and the Shimmer3 IMU.

Figure 2.4: The equipment that is needed to hold and fix the Shimmer3 IMU to the bike.

Steer angle

The steer angle cannot be measured directly by the IMU as this device measures angular velocity as opposed to angular orientation.

The steer angle is obtained by numerically integrating the relative angular velocity using the Matlab function cumtrapz(), which integrates the data using the trapezoidal method. The sampling frequency has been increased and fixed at 100 Hz for all trials to obtain more accurate results. Linear drift has been accounted for, more information about this process follows in section 2.4.4. This sampling frequency has been selected because the relative orientation between two IMUs could be determined with an absolute error of 0.5 degrees after 90 seconds in a pilot test where the initial and final orientations of the sensors were known. This shows that only two IMUs are required and are sufficient to measure the required data for this study.

Velocity

As explained before, all metrics require a constant velocity during the manoeuvre. Therefore, the velocity needs to be measured as well.

Applying a correction on the data for the real-time velocity throughout the whole trial is not reachable in the time span of this research. It has been decided that all trials with an average recorded velocity of $\pm$ 10% higher or lower than the selected average velocity are seen as invalid and discarded. A larger bandwidth would lead to trials that are less similar for comparison, and a smaller bandwidth would make it necessary to discard a large proportion of the trials that have to be discarded, which can lead to problems in the planning of this study.

As the maximum yaw factor is dependent on velocity, it is important to investigate the maximum recorded velocity of each trial as well. Thus, all trials with a maximum recorded velocity $\pm$ 10% higher or lower than the selected absolute velocity are discarded as well.

To ensure that a speed as constant as possible is maintained, the rider receives visual feedback on his velocity. The velocity of the vehicle is displayed to the rider with the phone application Strava Premium which measures and logs the velocity of the vehicle based on GPS. This velocity measurement is collected at 1 Hz and is used to discard the invalid trials. The data is solely used for the discarding of trials based on the mean and maximum of the velocity, therefore a GPS with a sample rate of 1 Hz is acceptable as a minimum. The next section will describe the track of the experiments in detail.

2.4.2. Track

The manoeuvres are performed on smooth concrete to reduce measurement noise. Additionally, the experiments are only conducted with dry pavement to avoid differences in traction during the different trials.

Slalom

The first track is for the slalom manoeuvre. The track is built from a cone trail for 40 meters where the cones are placed at a distance of 3 meters from each other, so in total 13 cones are present. It has been chosen to place the cones in a straight line, like the track of D'hondt et al., (2022) and Yu et al., (2016) [11, 40]. It is hypothesized that the differences in yaw factor between the vehicles are easier to detect with this track, compared to a trail of cones that are placed with a lateral offset.

10 meters of space for acceleration is added prior to the cone trail. Figure 2.5 shows a schematic view of the track.

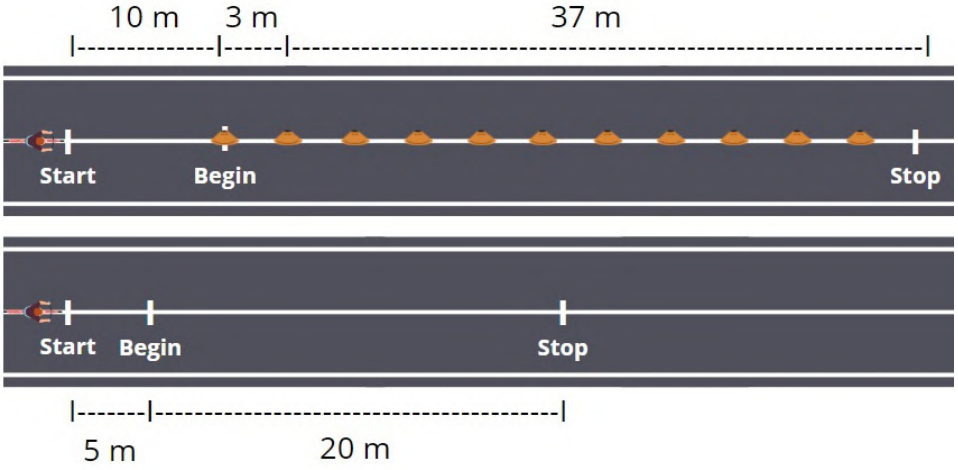

Figure 2.5: The track of the two manoeuvres, the top track is the slalom track and the bottom track is the low-speed line-following track.

The speed of the manoeuvre needs to be selected, which is dependent on the selected cone spacing. To activate the internal human controller the most, the manoeuvres are performed with a velocity that maximizes the difficulty. This tests the vehicles at their limit. The rider maintains a constant speed of 12 km/h, so a cone has to be passed approximately every second. This speed was found to be the maximum velocity at which the cones can still be avoided during the manoeuvre and which can still guarantee safety.

This paragraph discusses similar tracks as found in the literature to verify the cone spacing and the speed that I selected. The study of D'hondt et al., (2022) compares bicycles and tricycles as well during the slalom, with success. The setup of their track has only led to failures during the trials while testing vehicles with a wheelbase of two meters [11]. Their set-up has been similar with a cone spacing of 3 meters and a velocity of 10 km/h constantly for all vehicles. It is possible that their velocity is not high enough to test the vehicles at their respective performance limit. Yu et al., (2016) perform the same test, although they perform the slalom with a car on a velocity of 35 km/h with a cone spacing of 12 meters [40]. In their test, a cone is passed every 1.3 seconds compared to 1.12 seconds for the test of D'hondt and 0.97 seconds for the test in this thesis. The maximal difficulty is desired, therefore the selected cone spacing of 3 meters and selected velocity of 12 km/h is suitable.

Low-speed line-following

The second track is for the low-speed line-following. A straight line of chalk is applied to the concrete for 20 meters. Five meters of space for acceleration is added prior to the straight line. Figure 2.5 shows a schematic view of this track as well. The vehicle starts from a known position to know the steer angle accurately. This position is carefully drawn on the ground with chalk using a level.

For this designed track, the right average velocity needs to be selected again. The design of this track is comparable to the study of Kovacsova et al., (2016) [22]. In their research, elderly riders are compared to middle-aged riders, which can be a factor that raised the velocity of the performance limit of the riders without risking injuries.

The speed of their manoeuvre is 7 km/h, which has been decreased in this study to increase the difficulty and reach the performance limit. The rider maintains a constant speed of 6 km/h. This is the lowest speed that can be used while being able to follow the line.

2.4.3. Test protocol

This section contains the protocol for the handling tests conducted in this research. For repeatability of the experiments, all steps that are conducted in the handling tests are listed below.

To reduce the improvement of performance in between trials, the participant takes time to learn and ride the specific vehicle per test for as long as necessary until the performance does not improve anymore. Afterwards, the test can be performed with the following steps: For the slalom maneuver:

1. Place the cones at a distance of 3 meters from each other.
2. Measure 10 meters of space for acceleration and draw the initial position carefully using a level.
3. Position the vehicle in the starting position.
4. Start the front sensor first, start the rear sensor afterwards. Start the velocity recording and start accelerating to 12 km/h.
5. Perform the slalom while keeping track of the velocity. Manoeuvre as tight as possible around the cones. Keep a velocity that is as constant as possible.
6. Stop the velocity recording. Stop the front sensor first, and stop the rear sensor afterwards.
7. Repeat this process from step 3 until all trials have been completed.

As described in section 2.2, the score of the metric can be compared without a correction if there are equal velocity limits between vehicles. For the low-speed line-following:

1. Draw a straight line for 20 meters.
2. Measure 5 meters of space for acceleration and draw the initial position carefully using a level.
3. Position the vehicle in the starting position and keep a steer angle of zero.
4. Start the front sensor first, start the rear sensor afterwards. Start the velocity recording and start accelerating to 6 km/h.
5. Perform the line-following while keeping track of the velocity. Track the line as well as possible. Keep a velocity that is as constant as possible.
6. Stop the velocity recording. Stop the front sensor first, and stop the rear sensor afterwards. Keep a steer angle of zero when stopping the sensors.
7. Repeat this process from step 3 until all trials have been completed.

The number of trials that are required differs per experiment and type of vehicle, this will be elaborated upon in their respective chapters. The vehicles themselves are shown and discussed in their respective chapters.

2.4.4. Data analysis

This section explains how the data from the sensors need to be manipulated, processed, and analyzed such that conclusions can be drawn.

Sensor syncing

The data can be extracted from the sensors and can be uploaded to Matlab. The data of the sensors can be synced in time by means of the Unix timestamp of the sensors. The sensors make use of an internal clock that measures the time of each data point and the data of the sensors can be synced by matching the start time and the end time of the IMUs precisely during the post-processing in Matlab. To do so, the data points are removed when only one of the two sensors was turned on.

Data processing

To remove the drift error from the numerical integration of the steer rate, an offset has been subtracted from the signal before numerical integration. This signal was the difference between the yaw rate of the frame and the yaw rate of the handlebars. A non-zero measurement difference between the two sensors at rest was found to lead to a linear drift error after integration.

A Savitsky-Golay filter is a type of low-pass filter that has been applied to make the signal reasonably smooth and to remove the high-frequency noise from the signal. The main advantage of the Savitsky-Golay filter is its ability to remove noise or unwanted fluctuations from a signal while preserving its shape. Unlike other filters, such as the moving average filter, which simply averages adjacent data points, the Savitsky-Golay filter fits a polynomial of a certain degree to a subset of adjacent data points [3]. This subset of the data points that are evaluated is called the window width. This allows the filter to capture the local shape of the signal and has been found to be more effective at removing noise and preserving the overall shape and trends of the data. This filter does not filter based on a selected cutoff frequency.

A small window width is required to keep most of the tendency of the signal intact. The widow width has been increased starting from 1 data point up to a window width that is reasonably smooth without discarding important information by visual inspection. A final window width of 81 data points has been selected. A signal consists approximately of 2500 data points in total. The window width should always be an odd number. The default degree of the polynomial has been used, which is a second degree for Matlab.

The result of the maximum yaw factor yields data points that approach infinity, which is why a larger window width of 201 data points is applied for this data to obtain a signal that can be analyzed.

The time delay between the roll rate and the steer rate is in the order of milliseconds [5, 6, 14, 22]. The obtained data with a sampling frequency of 100 Hz needs to be interpolated to be able to obtain more data points to be able to conclude with higher accuracy on the exact amount of time delay in milliseconds. The Matlab function interp() has been used to obtain 30 times more data points for this metric.

Figures and information about the vehicles that are put through the handling tests can be found in the following chapters, even as the statistical tests that have to be conducted to answer the research question.

3

Chapter 3: Reference study

In this experiment, I performed the handling tests for multiple different bicycles, and I compared their performances. To be able to visualize the scores of the combined handling performances obtained in this thesis, I needed a reference scale where the handling performance of the vehicles will likely fall in between. The goal of this study is to select bounds for the normalization scale and to see how well the handling test method can distinguish between different vehicles. Ultimately, this will give insight into the resolution of the handling quality measurement method. I interpreted the obtained results using knowledge from literature to be able to conclude on the factors of the design of the vehicles that could have led to the obtained score in terms of the trail, head angle, and wheelbase.

3.1. Method

The protocol of the handling tests in section 2.4.3 was followed during the tests. This section covers the additional methodology that has been used to obtain the results.

3.1.1. Reference vehicle

As discussed in section 2.3.2, the bounds of the normalization scale have to be selected for visualization of the results. I choose a normal city bike as the average handling reference. This bicycle is the Batavus Verona 7. The bicycle is tested according to the protocol to determine this average handling point. The score on the handling performance is calculated, and this is afterwards scaled to the halfway point on the normalization scale, such the total score for the handling performance of the reference vehicle is set as 0.5. Then the reference bicycle is tested again, with the front fork flipped to significantly increase the trail. This also slightly decreases the head tube angle. The Batavus Verona has been selected for its good ability to flip the front fork without collisions with the frame or pedals. This handling score is selected as the worst handling for the scale. This way, the hypothesis is that the performance of all vehicles that are tested during this thesis will not be worse than the score of the Batavus with the flipped front fork. In addition, it is hypothesized that the score can be better than the reference bike, up to the score of the reference bicycle plus the difference with the score of the bicycle with the front fork flipped. The maximum of the [0,1] normalization scale is therefore the score of the reference bike plus the difference when the front fork is flipped, figure 3.1.

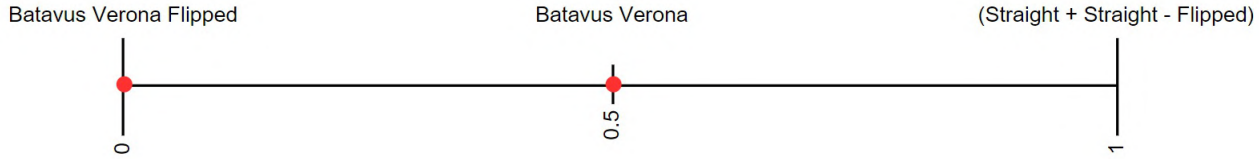

Figure 3.1: The normalization scale, based on the score of the reference vehicle.

The mechanical specifications of this reference bicycle can be found in table 3.1.

Table 3.1: The mechanical data of the bicycles that are tested during the reference test. The other vehicles will be introduced in the next section.

Vehicle	Wheelbase [m]	Trail [mm]	Head angle [°]	Tire width [mm]	Weight [kg]
Batavus Verona 7	1.20	35	68	40	19.5
Batavus Verona 7 - Flipped	1.20	155	66	40	19.5
Gazelle Ami C7	1.15	72.5	68	40	23.5
Giant Propel	1.02	116	69	30	8.5

To obtain accurate data on the handling of the reference vehicle, 15 trials have been performed on both of the manoeuvres.

Flipping the front fork is the first test to see if the handling metric can discriminate between different designs. This changes the trail, and this can therefore alter the handling performance of the vehicle. The hypothesis is that the handling performance score decreases by flipping the front fork and thereby increasing the trail from 35 mm to 155 mm. This can make the bike feel less agile, responsive, and controllable [31].

3.1.2. Other vehicles

More vehicles have been tested during the reference test, and the performances are compared. This provides information about the handling performance for a broader range of bicycles, and it can help to conclude the minimal resolution of the handling evaluation method. The Gazelle Ami C7 has been tested. This is the bicycle that has been converted into the Dressel tricycle, and it is required to know its handling performance before the transition. This way, the change in handling performance can be reported. The bicycle has electrical assistance. Yet, in the handling tests, the bicycle has been tested without assistance to be able to compare the performance with the other bicycles.

Furthermore, I tested a sportive Giant race bicycle to add performance information to the database and build more confidence in the method. The introduction stated that racing is not investigated, but it can be investigated whether the handling evaluation method is designed well for testing the performance of commuter vehicles, by looking at the performance of the Giant. All bikes can be seen in figure 3.2. Table 3.1 shows the important mechanical specifications of the vehicles that are compared.

(a) The Batavus Verona and the Gazelle Ami C7 [17]. Large similarities between the designs can be seen.

(b) The Giant Propel racing bike

Figure 3.2: All bicycles that have been tested during the reference study.

The vehicles are put through the same handling tests and the protocol of the handling tests is used. In total, 15 trials are needed in both manoeuvres to perform the tests on all vehicles. This means that a total of 150 trials are completed for all bicycles up to this point.

3.1.3. Statistical analysis

This section contains two parts, the statistical tests and analyses of the reference bicycle will be stated first. Afterwards, the analyses for the other tested vehicles are reported.

Reference bicycle

After the data is processed, the handling performance receives its score in the way that is described in the previous chapter. The goal of the first test is to create insight into the significance of the effect of flipping the front fork of the reference bicycle on the handling performance. This means that the same vehicle is compared, with the only change in design being a different trail. The handling performance of the Batavus Verona 7 with a flipped front fork is compared to the performance of the Batavus Verona 7 with a normal front fork. This gives insight into how well the method can distinguish between a single vehicle with a different design parameter.

To decide which statistical test can be used, it has to be checked if the results of all metrics follow a normal distribution. For each of the three experiments, the data of the trials are tested for normality using a Quantile-Quantile plot, (QQ-plot). A normal distribution is present if the data has a good fit with a straight line in the QQ-plot [16]. The QQ-plots have been created using the data processing and programming language Matlab. To confirm the normal distribution of the data, a Shapiro-Wilk test is done. A normal distribution is present if the P-values are larger than 0.05. In that case, the null hypothesis of a normal distribution can not be rejected.

For normally distributed data, the significance of the effect of flipping the front fork of the reference vehicle is investigated with a paired t-test. The null hypothesis is that the means of the two tested configurations are equal, and the alternative hypothesis is that there is a difference in the means.

The t-test is paired in this case because the data that are being compared are related. Specifically, the handling performance is being compared for a single subject, so the data is related because they come from the same subject.

The effect size of the flipping of the front fork has been calculated using Hedges' *g*. This parameter is comparable to Cohen's *d*, which gives an estimate of the effect size for normally distributed data. This parameter calculates how many standard deviations the means are away from each other. The Hedges' *g* corrects this value with a correction factor based on the number of samples N, as Cohen's *d* is biased upwards for small sample sizes [34]. Hedges' *g* is given by:

$$Hedges'g = \frac{M1 - M2}{\sqrt{\frac{SD_1^2 + SD_2^2}{2}}} \frac{N-3}{N-2.25}\sqrt{\frac{N-2}{N}} \tag{3.1}$$

The mean and standard deviation (SD) is reported for each metric of each of the two designs.

Other vehicles

For the other vehicles, it is important to know what the minimal resolution is of the method. For the two vehicles that have the closest handling performance, another t-test is performed to investigate if the handling scores on the metrics of the vehicles can be discriminated with statistical significance. For a rejected null hypothesis, the method can indicate on a significant level that the vehicles are not the same vehicle. When the results show insignificance, the vehicles with the next closest performances are compared to see when statistical significance can be found.

For all of the other vehicles, the mean and standard deviation is reported for each metric as well.

3.2. Results

This section reports on the results from the reference test, as described in the method section.

3.2.1. Reference bicycle

This section reports the results that have been found by testing the Batavus Verona, the reference bicycle, and the same bicycle with the front fork flipped. The results of the other bicycles that have been tested will be covered in the next section.

The two versions of the bicycle have been tested according to the protocol. The change in handling performance between the two versions could clearly be felt while running the tests.

The trials with an invalid velocity are discarded. The trials of the reference bicycle and their corresponding average velocity can be seen in figure 3.3. The data has been obtained with Strava GPS application that is used to compute the mean velocity during a trial.

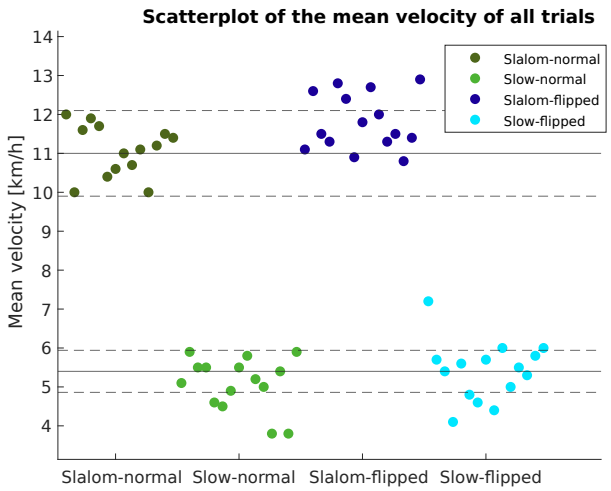

Figure 3.3: The mean velocities during all trials with the Batavus Verona 7 with the two manoeuvres and the front fork flipped.

It has been observed that a peak overshoot in the maximum absolute velocity of the slalom occurs. This means that it has been found that the vehicle could perform the manoeuvre faster. The bounds of the peak velocity have been raised and the trials are discarded for a peak velocity of 15 km/h $\pm$ 10%. This bandwidth has been discussed in section 2.4.1. A valid and an invalid trial with their absolute velocity are visualized in figure 3.4. The absolute velocity data throughout a valid trial, compared to an invalid trial, is shown in figure 3.4. The bounds are added that show the range where the maximum velocity should be in between.

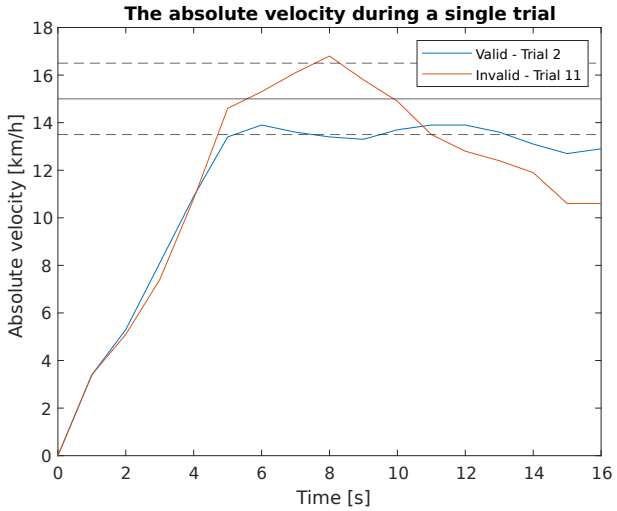

Figure 3.4: The absolute velocity of a trial with the reference through the duration of the trials. The acceleration period can be seen as well as a constant velocity during the trial.

After 15 trials with the reference bicycle for both manoeuvres, 10 valid trials remained for the slalom manoeuvre and 11 valid trials remained in the low-speed line-following manoeuvre. This is due to the sensors not measuring, or that the average or maximum velocity during the trial is not close enough to the selected speed. All velocity data of the other tested vehicles can be found in Appendix C.2.

After the data from the Shimmer sensors are exported, the data can be processed. Figure 3.6 shows the signals that have been used to calculate the mean absolute steer angle during the low-speed line-following. Although similar, the trials cannot be visualized altogether as the course of the trial is different for each performance. The steer angle after numerical integration over time can be seen in figure 3.5a. The time delay between the roll rate and the steer rate can be seen in subfigure 3.5b. This figure shows that the steer rate lags throughout the whole duration of the signal. Figure 3.6a shows the plot of the cross-correlation between the steer rate and the roll rate. More time series can be found in Appendix B.

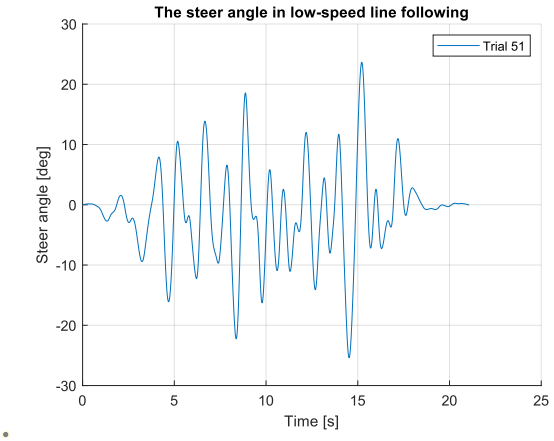

(a) The steer-angle of the handlebars of the Batavus Verona during a trial in the low-speed line-following manoeuvre.

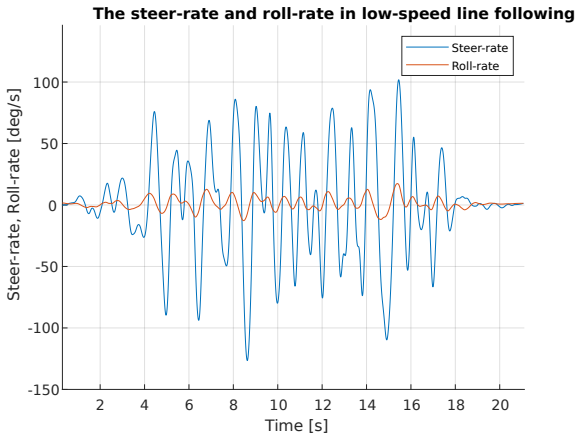

(b) The steer rate and the roll rate during a trial in the low-speed line-following manoeuvre.

Figure 3.5: Two of the processed signals from the data, plotted in Matlab.

Figure 3.6b shows the yaw factor over time. As the yaw rate and the steer angle have the same sign for almost the whole duration of the manoeuvre, the yaw factor is strictly positive while in the slalom. Peaks occur as sudden sharp turns are required, which shows the difficulty to handle the vehicle. A good yaw factor is low and has no large local peaks. For some trials, I observed local peaks (Appendix B). It has been found that the maximum yaw rate often occurs at the peak velocity, which is why it is important that the velocities and peak velocities throughout the trials are similar and the right trials were discarded.

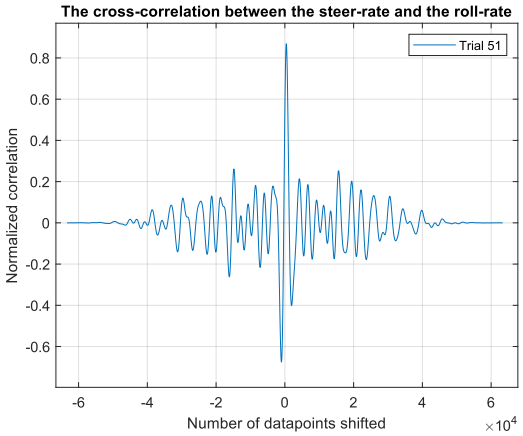

(a) The normalized cross-correlation between the roll rate and the steer rate. The X-axis indicates the number of data points that the signal needs to be shifted to obtain the peak in cross-correlation. For this trial, the number of data points with the maximum correlation (421), represents a time delay of 140 milliseconds. This data originates from trial 51 with the Batavus Verona with a flipped front fork.

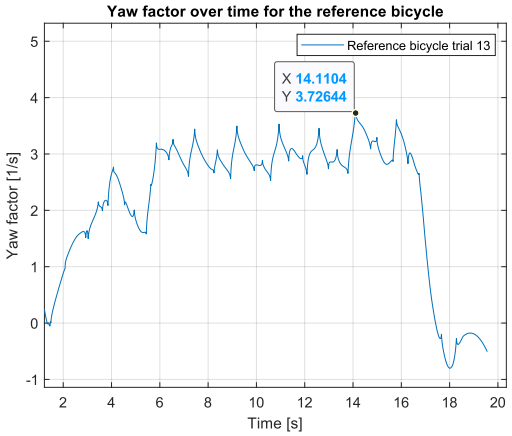

(b) The yaw factor against time for the Batavus Verona. The peak of the yaw factor can be seen. For this trial, the maximum yaw factor = 3.73. Throughout the slalom, the sign of the yaw factor is strictly positive. Peaks occur when sudden changes in direction are required to perform the slalom and avoid a cone. This data originates from the Batavus Verona in trial 13 with a normal front fork.

Figure 3.6: Two of the processed signals from the data, plotted in Matlab.

For the reference vehicle, The computed results of the metrics throughout all trials are shown in table 3.2:

Table 3.2: The obtained results of the metrics in all valid trials for the Batavus Verona 7 with a normal front fork, and a flipped front fork respectively. The invalid trials are not included in this table, 4 trials for the reference bicycle with a normal front fork and 5 trials for the reference bicycle with a flipped front fork.

Trial number	Max. Yaw factor Normal [1/s]	Max. Yaw factor Flipped [1/s]	Avg. Abs. Steer angle Normal [°]	Avg. Abs. Steer angle Flipped [°]	Avg. Time Delay Normal [s]	Avg. Time Delay Flipped [s]
1	4.32	3.87	3.67	7.06	0.0881	0.215
2	3.67	4.04	4.13	7.65	0.0915	0.186
3	3.44	3.86	3.11	8.47	0.0948	0.165
4	3.92	5.55	3.61	7.41	0.113	0.140
5	3.43	3.99	3.54	6.75	0.117	0.163
6	3.55	3.96	4.34	7.49	0.0655	0.165
7	3.76	4.35	3.62	8.07	0.113	0.153
8	3.43	4.28	3.48	7.85	0.0911	0.137
9	3.29	4.55	3.69	5.77	0.0798	0.131
10	3.24	4.08	4.08	5.57	0.0911	0.115
11	-	-	3.01	8.03	0.107	0.147
Mean	**3.60**	**4.25**	**3.66**	**7.28**	**0.096**	**0.16**
SD.	**0.31**	**0.48**	**0.39**	**0.88**	**0.015**	**0.026**

The total score of the Batavus can be calculated according to equation 2.6. This leads to a score of 1.20 for the Batavus with the normal front fork, and 0.617 for the Batavus with the flipped front fork. As stated before, these numbers are used to scale the normalization. This means that a decrease has been found in handling performance when comparing the scores. It can be concluded that the novel handling performance evaluation method that is provided can distinguish the handling performance of multiple different designs and the outcome is as expected.

To visualize the breakdown of this score in the score of the three metrics, a radar chart with the scores of the metrics of the reference vehicle with a normal and a flipped front fork can be seen in figure 3.7. The axes have been scaled with the same scale factors as explained in section 2.3.1, to show the scores of the metrics with the same order of magnitude. A large surface indicates high performance and a low score on the metrics leads to a small surface in the radar chart.

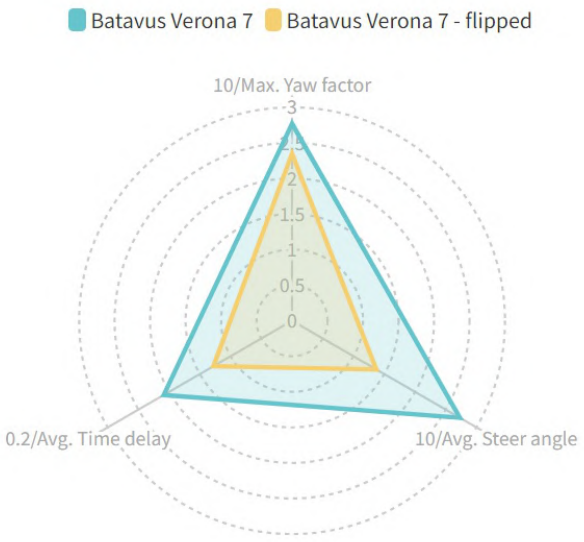

Figure 3.7: The performance of the two versions of the Batavus bicycle. Each axis represents the score of one metric. The reciprocal of the mean is used and the score is scaled with the corresponding scale factor. A large surface indicates a high performance.

This figure shows also the decreased handling performance of the reference bicycle when the front fork is flipped. On each of the three metrics, a lower score is obtained which leads to a decreased surface in the radar plot.

The QQ-plots of the resulting data in the tests show a normal distribution. Figure 3.8 shows the QQ-plot of the data of the three metrics for the reference bicycle with a normal front fork. The straight line implies a normal distribution.

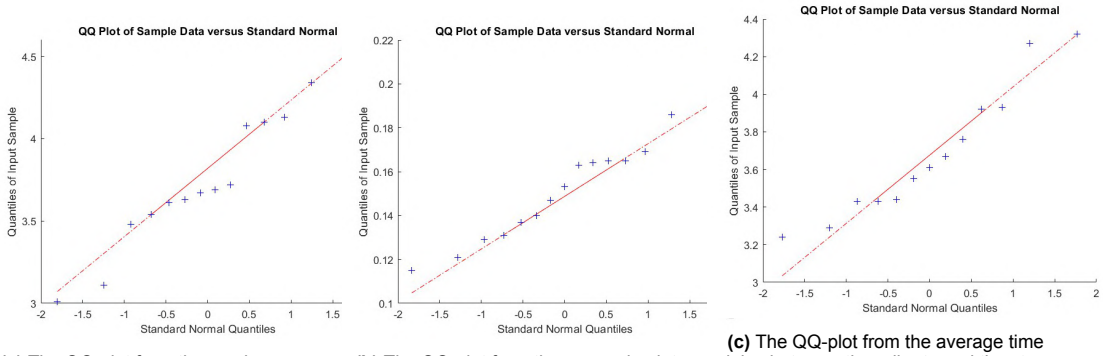

(a) The QQ-plot from the maximum yaw factor.

(b) The QQ-plot from the mean absolute steer angle.

(c) The QQ-plot from the average time delay between the roll rate and the steer rate.

Figure 3.8: The three QQ-plots from all three metrics for the reference bicycle with a normal front fork. All three show similarities with a straight line.

To prove normality in a second way, the Shapiro-Wilk test can provide a P-value that checks for normality. Table 3.3 shows the P-values. P-values need to be larger than 0.05 for a significance level of 5%, to prove normality. This proves that a normal distribution is present. Therefore, the statistical tests can be performed with parametric tests. Each time before the statistical significance is calculated, this assumption is checked.

Table 3.3: The P-values of the Shapiro-Wilk test, which can test for a normal distribution of the data.

Metric	P-value
Max. Yaw Factor	0.23
Avg. Steer angle	0.62
Avg. Time Delay	0.53

To see the statistical significance of the effect of flipping the front fork on the handling performance, two-tailed paired t-tests are performed with a significance level of $\alpha = 0.05$. Table 3.4 reports the P-values for each metric. The data, means and standard deviations can all be found in table 3.4.

Table 3.4: The P-values of the t-tests. All P-values are smaller than 0.05. Therefore the results show a significantly lower handling performance score when the front fork is flipped.

Metric	P-value
Max. Yaw Factor	0.005
Avg. Steer angle	<0.001
Avg. Time Delay	<0.001

The P-values show that the decrease in handling performance by flipping the front fork of the Batavus reference vehicle is significant. The effect sizes can be reported from the results of the calculated Hedges' *g*. The results are found in table 3.5

Table 3.5: The effect sizes of flipping the front fork of the Batavus reference vehicle for each of the three metrics.

Metric	P-value
Max. Yaw Factor	1.29
Avg. Steer angle	4.25
Avg. Time Delay	2.39

Effect sizes of 0.2 indicate a low effect, effect sizes of 0.5 indicate a medium effect, effect sizes of 0.8 indicate a large effect, and effect sizes that are larger than 1 indicate a very large effect according to Cohen (2013) [8]. Therefore, the effect of flipping the front fork of the Batavus reference bicycle on the handling performance is very large.

3.2.2. Other vehicles

This section contains the results of the handling tests of the Gazelle Ami C7 and the Giant Propel. A bicycle with a large negative trail has been tested as well, but no clear conclusions could be drawn from the data of this bicycle. More information on this bicycle can be found in Appendix A. So far, the handling evaluation method has shown to be able to discriminate between the two versions of the reference bicycle. Table 3.6 shows the score per metric and gives the total normalized score of each bicycle. The score of the reference bicycle, the Batavus Verona, is included again to be able to compare the scores. The data from all single trials can be found in Appendix C.

Table 3.6: The mean and standard deviation for each metric and total normalized score for the vehicles that have been tested during the reference test.

Vehicle	Max. Yaw factor Mean [1/s]	Max. Yaw factor SD. [1/s]	Avg. Abs. Steer angle Mean [°]	Avg. Abs. Steer angle SD. [°]	Avg. Time Delay Mean [s]	Avg. Time Delay SD. [s]	Total score
Batavus Verona 7	3.61	0.31	3.66	0.39	0.0956	0.015	**0.5**
Gazelle Ami C7	4.09	0.25	3.96	0.59	0.0796	0.036	**0.49**
Giant Propel	4.31	0.45	3.68	0.62	0.136	0.016	**0.30**

Similarly to the reference vehicle, the scores of the separate metrics can be compared and visualized in a radar chart, figure 3.9. The reference bicycle, the Batavus Verona, has also been included in the radar chart to compare performance.

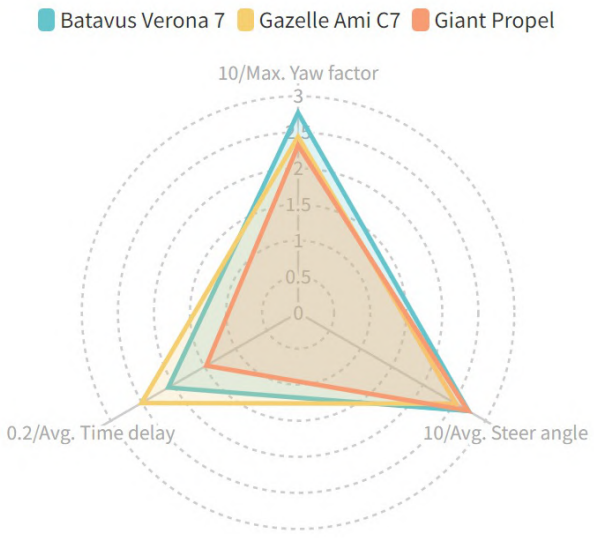

Figure 3.9: The performance of the reference bicycle, the Gazelle Ami C7 and the Giant Propel in a radar chart.

The scores of the vehicles can be added to the normalization scale and this is visualized in figure 3.10.

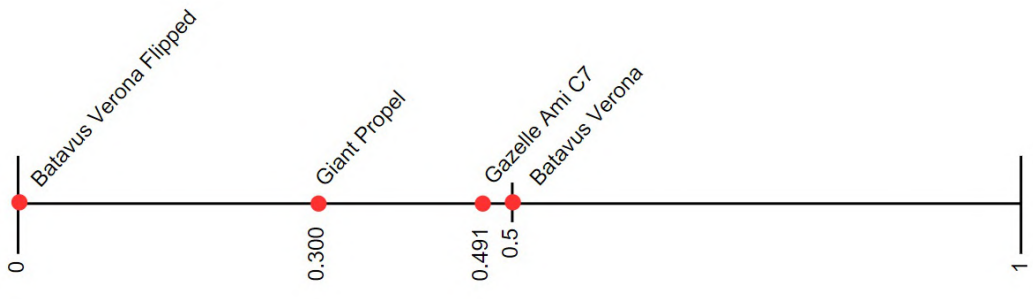

Figure 3.10: The performance of the vehicles on the normalization scale.

The two-tailed paired t-test between the performance of the Batavus Verona and the Gazelle Ami C7 shows that the yaw factor is significantly different, t(9) = 3.34, p = 0.01. For a significance level $\alpha = 0.05$, the mean absolute steer angle is not significantly different between the two bicycles, t(9) = 1.36, p = 0.21. The time delay is also not significantly different, t(9) = 0.89, p = 0.39 this means that the closely related design of the bicycles leads to a performance that can be discriminated on moderate speed, but not on low speed.

For more different designs, the Batavus Verona and the Giant, the two-tailed paired t-test shows also a significant difference in the average time delay between roll rate and steer rate (t(9) = 3.82, p = 0.008) but no significant difference in mean absolute steer angle, t(9) = 0.44, p = 0.67.

3.3. Discussion

The results show that all three metrics decrease significantly in performance when the front fork of the reference bicycle is flipped. This means that the metrics detect a lower handling performance and it can be stated with certainty that the reference bike with a normal and flipped front fork is not the same design. This means that the method is valid and can be used to see the differences in handling performance between the configurations of the Dressel tilting tricycle, in a later part of this thesis.

For the Gazelle Ami C7, the radar chart shows that the handling performance of the bicycle is very similar to the reference vehicle, both being city traffic commuter vehicles. All metrics obtain similar scores. The Gazelle has slightly better low-speed handling performance and slightly decreased performance in the slalom. Similar geometries and mechanical specifications will have led to this comparable performance score.

The t-tests show that it is only partially possible to discriminate between the Batavus and the Gazelle for multiple metrics. It can be stated that the method can discriminate between bicycles with a more clear difference in design, or either that more data in the trials is needed to decrease the standard deviation further. It has been shown that differentiating between very similar designs is most difficult for the metric that uses the mean absolute steer angle.

It is important to state that the means of the obtained results can be determined with more certainty if the number of trials is increased further in future research. When ranking vehicles with small differences in design, this is an important aspect. As the handling performance of the Gazelle Ami C7 is close to the performance of the Batavus Verona, the ranking can become significant when adding many trials.

A good performance was expected of the well-built and expensive Giant Propel. However, a decreased performance is obtained for the Giant Propel. This bent-over race bicycle has shown to be more difficult to steer in the slalom and has lower responsiveness than the other tested city bikes in this study. The trail of the Giant is higher, the wheelbase is smaller and the position of the rider is different than the other bicycles, which could be an explanation for the obtained results. These results can also be explained because the vehicle is built for riding at higher speeds with larger corners, and these moderate-speed and low-speed maneuvers are not the optimal environment for the bicycle. The vehicle is not the optimal design of a commuter vehicle for city traffic. Therefore, the score has turned out lower than the other city bikes in this test. This also indicates that the manoeuvres that are selected function well in scoring high for commuter vehicles in city traffic, and lower for vehicles with other purposes.

4

Chapter 4: Tricycle comparison

Now that it has been confirmed that the handling performance of different vehicles can be measured and distinguished, the next step to ultimately be able to answer the research question is to test the method on tilting tricycles.

4.1. Method

This experiment involves two tricycles of Noordzij, the designer and manufacturer of the two tilting tricycles. In this experiment, the goal is to measure the performance of his tricycles and compare the score to see if the handling performance metric can also discriminate between these types of vehicles and to see if the total score has the potential to transcend the score of bicycles. A top view and a front view of the tricycles can be seen in figure 4.1a and 4.1b, respectively.

According to the designer and manufacturer, it is difficult to express the mechanical properties of the vehicles in conventional trail and head angle, due to the custom design. The green tricycle, the far one in figure 4.1, has been designed with a custom steering rod and a steering knuckle. The estimates of the mechanical properties are given in table 4.1.

(a) A top view of the tricycles.

(b) A front view of the tricycles

Figure 4.1: The two tricycles of Piet Noordzij. The silver tricycle is referred to as Test Tricycle 1 and the green tricycle is referred to as Test Tricycle 2.

Table 4.1: The mechanical properties of the two tricycles that have been tested.

Vehicle	Wheelbase [m]	Trail [mm]	Head angle [°]
Batavus Verona 7	1.20	35	68
Test tricycle 1	1.10	80	70
Test tricycle 2	1.10	80	72

4.1.1. Axle track

One key difference between tricycles and bicycles is the axle track of the two front wheels. For the low-speed line-following, this does not make a difference in the trajectory of the manoeuvre. However, for the slalom, this changes the trajectory.

Due to an increased axle track, tricycles need to cover more distance along a different trajectory than the equivalent bicycles. However, it is unknown what the effect of the increased axle track is on the maximum yaw factor, that is related to the controllability of the steering. Therefore, an additional experiment needs to take place to investigate the effect of a wider axle track on the maximum yaw factor metric. If the maximum yaw factor is dependent on the axle track, a correction factor needs to be made or the trajectory needs to be altered.

By shifting the cones of the slalom track with a known lateral offset, the trajectory of a tricycle with the same axle track can be recreated for the reference bicycle, the Batavus Verona. The front wheel now has to follow the same path as the equivalent tricycle. I call this offset the virtual axle track. The rear wheel is unrestricted, as it would have been for the tricycle in tadpole design. This means that the rear wheel does not have to pass the cones from the outside. I put the reference bicycle through the handling tests for a virtual axle track of 200 mm, 400 mm, and 600 mm, to conclude on the effect on the maximum yaw factor. The modified track can be seen in figure 4.2. A possible trajectory of the vehicle is included in the figure.

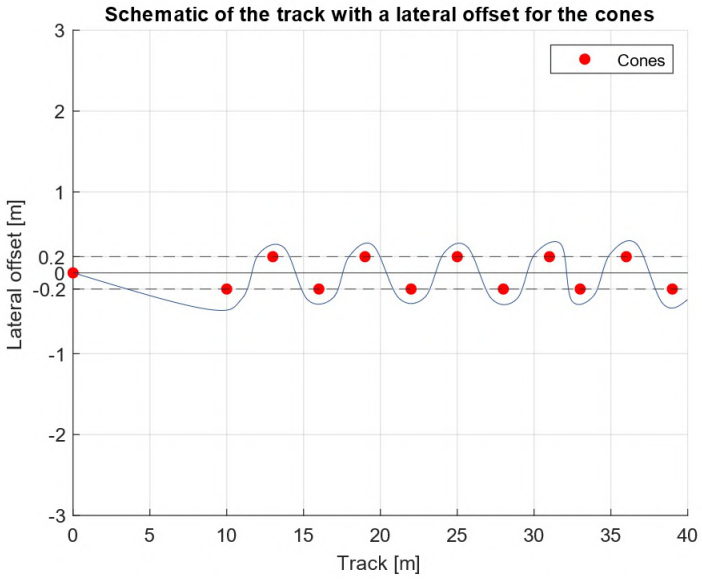

Figure 4.2: The modified track from a top view. The bicycle needs to pass the cones from the outside. A possible trajectory of the bicycle is shown.

4.1.2. Experimental method

Once I investigated the effect on the maximum yaw factor, the handling tests can start using the protocol described in section 2.4.3. The rider puts both vehicles through 10 trials in both manoeuvres, as opposed to 15 trials in the reference study as the test location is not in Delft. This saves limited time.

4.2. Results

The results are reported in this section. This section provides a detailed analysis of the yaw factor test first, to offer insights into its effect on different axle tracks. The next subsection will report on the results of the handling tests with the two tricycles.

4.2.1. Yaw factor test

Figure 4.3 shows the obtained maximum yaw factors for each virtual axle track that has been tested by shifting the cones with a known lateral offset.

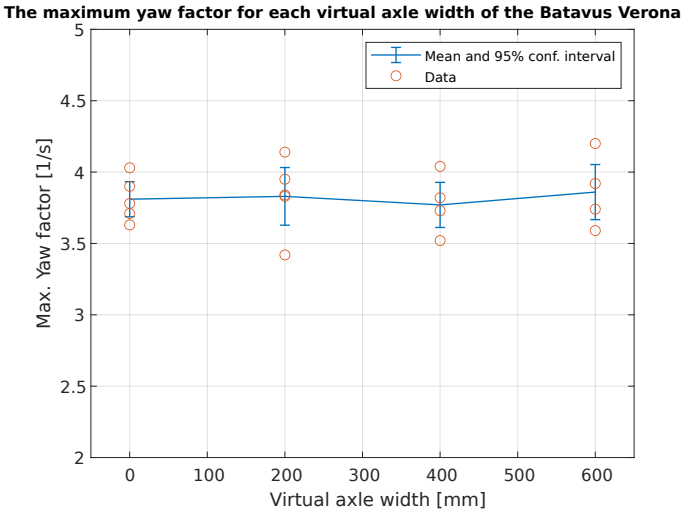

Figure 4.3: The resulting maximum yaw factors for all trials with the virtual axle tracks and their corresponding 95% confidence interval.

It can be seen that with a 95% confidence interval, the means of the different virtual axle tracks do not differ for the maximum yaw factor. Therefore, the maximum yaw factor is independent of the axle track and only gives an indication of the controllability and smoothness of the steer response during the manoeuvre. This means that the tricycles with different axle tracks can also be tested using the slalom manoeuvre with the same track as the bicycles. This means that the obtained differences in results between the different vehicles are created because of the other design parameters, such as the wheelbase, trail, mass distribution, or manufacturing quality.

4.2.2. Handling test results

Because the yaw factor is independent of the axle track, the score of the metrics can be calculated without adding a correction factor. I, therefore, determine the result of the three metrics in the same way as has been done in the reference test. Table 4.2 shows the score per metric and gives the total normalized score of each tricycle, normalized. The score of the reference bicycle, the Batavus Verona, is included again to be able to compare the scores.

Table 4.2: The mean and standard deviation for each metric and total normalized score for the tricycles that have been tested during the reference test.

Vehicle	Max. yaw factor Mean [1/s]	Max. yaw factor SD. [1/s]	Avg. Abs. Steer angle Mean [°]	Avg. Abs. Steer angle SD. [°]	Avg. Time Delay Mean [s]	Avg. Time Delay SD. [s]	Total score
Batavus Verona 7	3.61	0.31	3.66	0.39	0.096	0.015	**0.5**
Test Tricycle 1	4.19	0.21	3.56	0.59	0.079	0.016	**0.52**
Test Tricycle 2	4.81	0.11	3.41	0.36	0.083	0.033	**0.47**

Similarly to the reference vehicle, the scores of the separate metrics can be compared and visualized

in a radar chart, figure 4.4. The reference bicycle, the Batavus Verona, has also been included in the radar chart to compare performance.

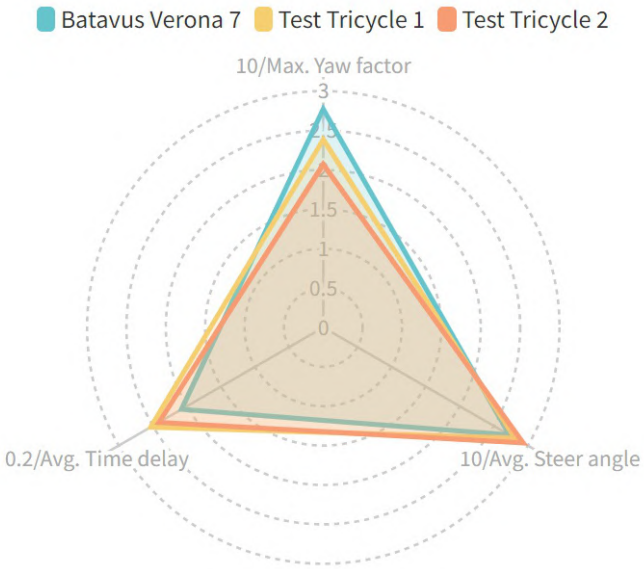

Figure 4.4: The performance of the reference bicycle, and the two tested tricycles.

The scores of the tricycles can be added to the normalization scale and this is visualized in figure 4.5.

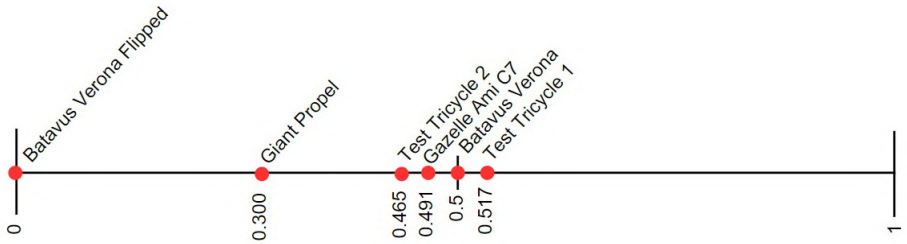

Figure 4.5: The performance of the tricycles added to the normalization scale.

4.3. Discussion

Interestingly, the score of the first tricycle that has been tested is higher than the reference bicycle. This means that improvements on a regular commuter bicycle for city traffic can be made in terms of handling quality. The second tricycle has a decreased performance. The manufacturing was not solid and this was felt during the maneuvers.

While the total score on the handling performance is similar for the tricycles and the reference bicycle, there are more clear differences when looking at the radar chart. It is interesting that the performance on the low-speed line-following manoeuvre has improved for the tricycles, while the performance on the slalom has decreased. The tricycles had some internal friction in the tilt mechanism, which can slow the tilt rate, which can make the line-following easier. The prototypes of the tricycles were not as easy and controllable to steer because of their manufacturing quality, which is why their slalom performance could have decreased. The same friction in the mechanism could have caused this as well. The method gives a clear insight into the strong and weak points of the vehicle and the test is successful. This section compared two tricycles. In the next chapter, I use the method to investigate the differences in the handling performance between multiple configurations of the Dressel tricycle.

5

Chapter 5: Optimal handling of the Dressel tricycle

The previous chapters have shown the capability of the method to evaluate handling performance between vehicles, both bicycles and tricycles. In this chapter, I used the handling evaluation method to test the finished prototype of the Dressel tricycle. A tilting tricycle has been designed by Dressel that makes use of an adjustable tilt mechanism. The next section will explain the working of this tilt mechanism in detail. The total realized prototype of the tilting tricycle can be seen in figure 5.1.

(a) The complete tricycle.

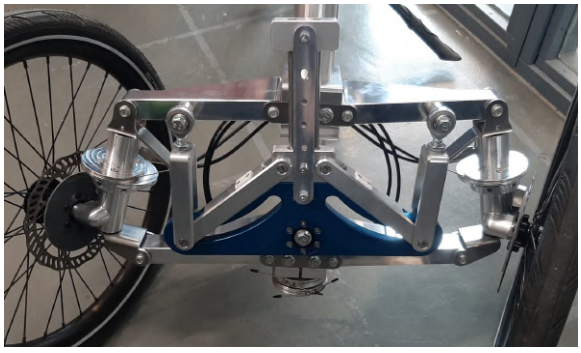

(b) The tilt mechanism of the realized tricycle.

Figure 5.1: The realized tilting tricycle as manufactured by DEMO.

5.1. Tilt mechanism

As mentioned before, the tilt mechanism of the tilting tricycle is composed of a combined parallelogram and a bell crank mechanism. The vehicle makes use of a split parallelogram with tilting of each side coordinated by a bell crank. The A-arms function as the parallel parts of the parallelogram. The tie rods connect the A-arms to the bell crank. The bell crank has a slot in which the tie rod ends can move to vary the connection points. Figure 5.2 shows the important parts of the tilt mechanism.

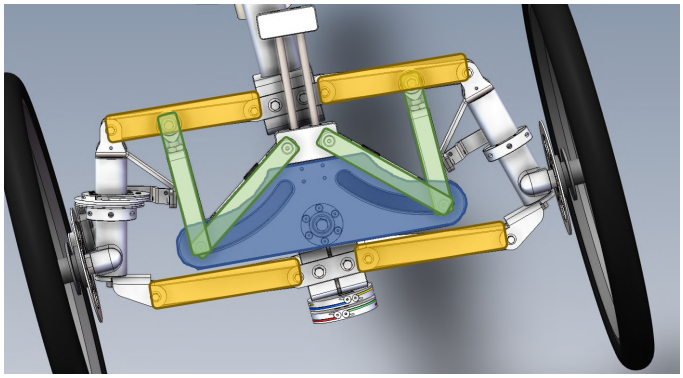

Figure 5.2: A Zoomed-in version of the SolidWorks model of the tilt mechanism of the tilting tricycle. In yellow, the A-arms can be seen. In green, the tie rods are visualized and the bell crank is highlighted in blue.

The connection point of the tie rods to the bell crank can vary by pulling the connection rod upwards. This changes the angle of the tie rods, henceforth referred to as the tie rod angle. This tie rod angle determines the characteristic tilt behaviour of the tricycle. A larger tie rod angle makes the tilt trajectory of the tricycle follow the path of a taller bicycle, which therefore slows down the roll. Parallel tie rods lead to the most tilt freedom and the characteristic of an equivalent bicycle. Tie rods that are shifted fully inwards will make the tilting tricycle rigid, like a regular tricycle. This is because the tilt limit also decreased up to fully rigid for tie rods that are shifted fully inwards.

Five connection holes for fixing the tie rod angles have been drilled into the tilt mechanism of the Dressel vehicle. The tie rod angle changes by connecting the bolt to a higher connection hole. Therefore, five configurations are testable that range from parallel tie rods to tie rods shifted fully inwards. Figure 5.3 shows what the tilt mechanism looks like for different connection points of the tie rods to the bell crank. The five connection holes can be seen.

Figure 5.3: The tilt mechanism of the Dressel tilting tricycle for tie rod angles of 0%, 25%, 50% and 75%, respectively.

5.2. Method

The goal and the procedures of the experiments with the Dressel tilting tricycle are explained in this section. The protocol of the handling tests (section 2.4.3) was followed during the tests.

5.2.1. Velocity compensation

It is previously explained that to compare the maximum yaw factor, all vehicles have to be tested at the same velocity, which has been the case so far. The theoretical expression of the yaw factor (equation 2.5) can be used to correct the yaw factor with a known parameter for a possible difference in velocity limit.

It is possible that altering the configuration of the tilt mechanism will change this maximum speed limit of the Dressel tilting tricycle while performing the manoeuvres.

It is important to investigate the resemblance between the obtained data during the slalom manoeuvre, and the data that would be obtained with the theoretical expression. With a high resemblance, this method can be used to scale the factor for comparison at different speeds. In other words, the obtained yaw factor should match the theoretical expression.

To investigate this effect, I took all trials from the reference study and the obtained yaw factor is compared to the theoretical yaw factor, using the raw data of the velocity, steer angle, steer rate, and the mechanical properties of the vehicle. The velocity and kinematic data are taken when the yaw factor is the highest. Also, the wheelbase, trail, and head angle are required parameters to calculate the theoretical yaw factor.

The mean percentile difference and the mean absolute difference are reported from the yaw factor results of the reference bicycle.

I performed another test to investigate the relation in more depth. Equation 2.5 shows that a linear dependency on velocity is expected. This relation can be measured by performing the slalom manoeuvre with the reference bicycle, for numerous different velocities. This can conclude on the resemblance of the obtained data with the theoretical expression as well. If a linear relation is found, the theoretical expression can be used to scale the factor for comparison at different speeds. If a non-linear relation is found, the obtained curve can be used to understand the bias of the correction factor for different speeds. According to equation 2.5, the theoretical slope is equal to $\frac{Cos(\lambda)}{w}$, the cosine of the head angle divided by the wheelbase.

5.2.2. Experimental method

In this study, I tested the finished tilting tricycle to evaluate which configuration of the front assembly leads to optimal handling performance. The tie rod angle can be changed by connecting the bolt in figure 5.3 to a higher point. The tie rod angles are the only parameter that can be changed in this prototype of the Dressel vehicle. The optimal handling performance are calculated by evaluating the handling performance of the first four configurations, as the last configuration offers no more tilting possibilities and this thesis investigates the tilting tricycle and not rigid tricycles.

The tie rod angle is a continuous independent variable, so this variable needs to be sampled in the range between its minimum and maximum, [0,45] degrees, from now on referred to as [0%,100%]. To be able to obtain a large enough sample size for each configuration, no more than four configurations can be tested with 15 trials in each configuration. Tie rod angles of 100% are not measured as this study is about tricycles with tilt capacity to at least some extent. Therefore, the continuous variable is sampled in five steps with a step size of 25% per evaluation. I only tested the first four configurations. This experiment leads to 120 trials in total for both manoeuvres while following the test protocol.

The results of this study include the following:

- The configuration of the Dressel tricycle with the respective optimal handling performance.
- The difference in handling performance between the Gazelle Ami C7 and the configuration of the Dressel tricycle with a 0% tie rod angle.

5.2.3. Statistical analysis

To investigate the statistical significance of the differences in performance between the configurations, I performed a one-way repeated measures ANOVA that compares all configurations for each of the three metrics. Because the metrics are unrelated, measured in different trials, and have a different order of magnitude, it is not possible to do a three-way ANOVA of all metrics at once. As the effect of one metric is investigated at a time, the ANOVA is one-way. As the study is within-subject, a repeated measures ANOVA is performed to correct for paired data. The null hypothesis is that all means of the configurations have the same performance per metric. Post-hoc tests are performed to investigate the pairwise significance of changing the tie rod angles with each step for all metrics. A Bonferroni correction is made to reduce the chance of type-1 errors, which are more likely to occur for a group of multiple pairwise investigations [1].

I investigated the effect of the transition from bicycle to tricycle as well, by performing a t-test with the result of the three metrics from the Gazelle before the transition and the tricycle after the transition.

5.3. Results

This section contains the results from the handling tests. These results are used to conclude the configuration with optimal handling performance.

5.3.1. Velocity compensation

The maximum yaw factor results are compared with the theoretical values obtained with equation 2.5. The obtained yaw factor results match the theoretical values with a deviation of 3.3% and have a mean absolute deviation of -0.17 points. The theoretical number uses the velocity, steer rate, and steer angle at the time with the maximum yaw factor. This theoretical number has a bias towards lower numbers.

The second test can provide additional information. The slalom performance has been measured with the reference bicycle for random velocities and the results are plotted in figure 5.4. A second-order least squares polynomial has been fitted through the data, this can investigate the linearity of the slope. Second-order relations are also used in the study by Zellner and Weir, (1979) [42]. The theoretical linear relation with a slope of $\frac{Cos(\lambda)}{w}$ has been added to the plot. A close resemblance to the theoretical relation has been found.

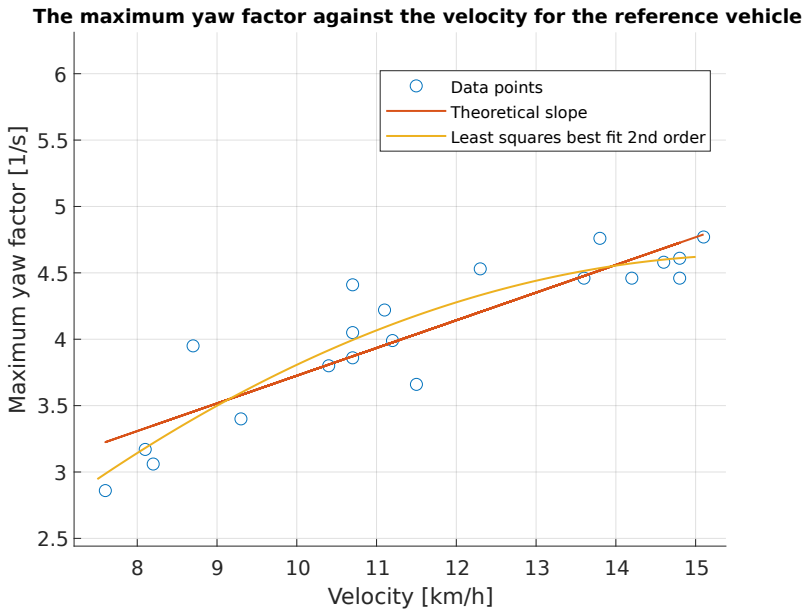

Figure 5.4: The relation between the obtained maximum yaw factor and the forward velocity of the vehicle. The second-order least squares best fit can be compared with the theoretical slope of the relation. The velocity has been taken at the time that the maximum yaw factor occurs.

For low speeds, it can be seen that the slope of the least squares fit is steeper than would be expected from the theoretical equation. This means that the scores of vehicles with a lower velocity limit result in better scores than the real handling should receive. This is also concluded by the negative bias in the previous test. This result means that it is possible to use the theoretical expression to scale the yaw factor for different velocities. However, the lower the maximum speed of the vehicle gets, the less accurate the obtained score will be. As the vehicle is not physically capable of performing the manoeuvre with the desired velocity, this is an extra disadvantage. It is impossible to report the true slope and shape of the relation between the yaw factor and velocity, as the scores are also influenced by the performance of the single trials.

The maximum yaw factor is reported with the compensated value, together with the time to complete the manoeuvre in the next section.

5.3.2. Handling performance

After the tests have been completed with all configurations, the data is analyzed. The results from the handling tests with the different configurations are reported in table 5.1. TT1 represents the first configuration with a tie rod angle of 0%. For TT2, the tie rods have been moved inwards with 25%. For TT3, the tie rods have been moved inwards with 50%, and for TT4 the tie rods have been moved inwards with 75%. The performance of the original Gazelle Ami C7 has been added for comparison.

Table 5.1: The mean and standard deviation for each metric and total normalized score for the different configurations of the tilting tricycle during the handling tests.

Vehicle	Max. Yaw factor Mean [1/s]	Max. Yaw factor SD. [1/s]	Avg. Abs. Steer angle Mean [°]	Avg. Abs. Steer angle SD. [°]	Avg. Time Delay Mean [s]	Avg. Time Delay SD. [s]	Total score
Gazelle Ami C7	4.10	0.25	3.95	0.59	0.079	0.036	**0.49**
TT1	4.42	0.39	4.79	0.56	0.097	0.030	**0.32**
TT2	4.12	0.13	2.57	0.48	0.078	0.022	**0.65**
TT3	4.37	0.51	2.33	0.36	0.046	0.017	**0.86**
TT4	4.63	0.74	1.33	0.32	-	-	**-**

The fourth configuration with tie rod angles of 75% could not obtain a score for the time delay between the roll rate and the steer rate as the stiff vehicle operated for a long time on the tilt limit. This is why the correlation between the roll rate and the steer rate is decoupled. Consequently, no total score could be assigned for the combined metrics for this configuration.

Contrary to the reference test, more configurations are compared for this study. Because of that, the results are not visualized in a radar chart as the overlaying triangles can make the results difficult to interpret. In the figures below, a stacked bar chart shows the difference in performance in the metrics for all configurations. The performance of the original Gazelle Ami C7 has been added for comparison.

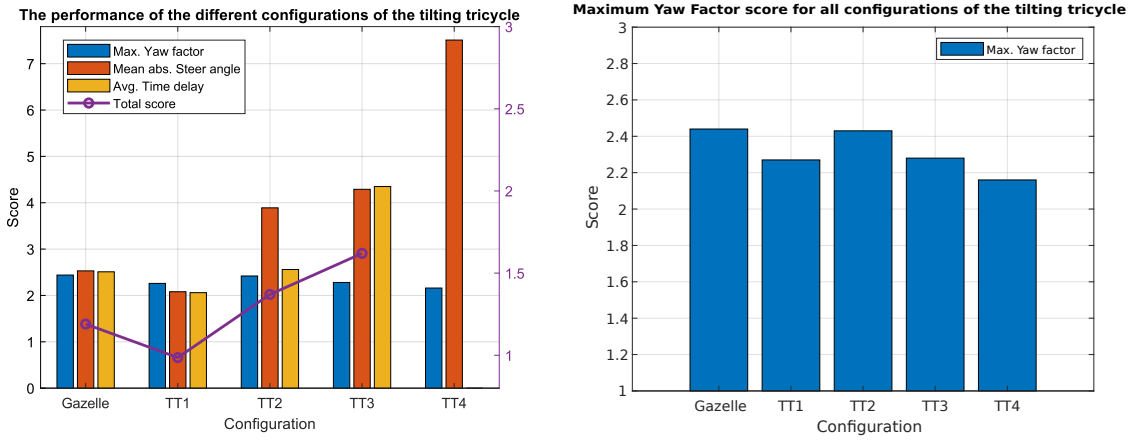

(a) The grouped bar chart of the performance of the configurations. The line shows the total combined handling performance

(b) The bar chart of the performance of the maximum yaw factor during the slalom manoeuvre.

Figure 5.5: The results of the handling performance metrics in bar charts.

The normalization scale can now be completed with the data from the configurations of the Dressel tilting tricycle. The nomenclature on the line in figure 5.6 is added corresponding to the names of the configurations in table 5.1.

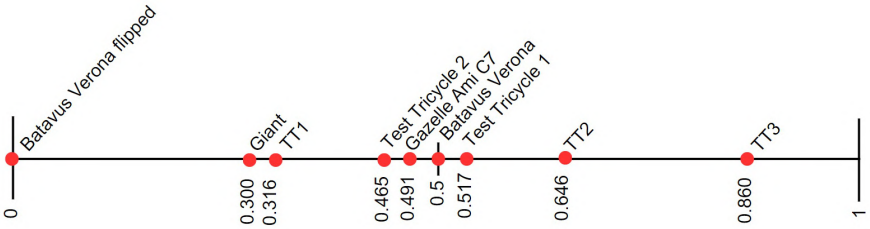

Figure 5.6: The complete normalization scale with the score of the configurations of the Dressel tilting tricycle added to the line.

The mean time to complete the slalom trial is reported below in table 5.2. This data is used to conclude the maneuverability of the vehicle as well next to the data of the maximum yaw factor. By increasing the tie rod angle to 75%, the mean time to complete the slalom trials increases which shows a decreased maneuverability.

Table 5.2: The mean time to complete the slalom manoeuvre for each configuration.

Vehicle	Mean time [s]
Gazelle Ami C7	16.5
TT1	18.9
TT2	18.3
TT3	18.4
TT4	26.5

5.3.3. Statistics

First of all, the performance of the tricycle with parallel tie rod angles is compared to the performance of the Gazelle bicycle before the transition. The maximum yaw factor has increased significantly, $T(8) = 4.99$, $p < 0.001$. The mean absolute steer angle has increased significantly, $t(8) = 2.93$, $p = 0.009$, but the time delay has not changed significantly, $t(8) = 0.92$, $p = 0.37$.

The performance of the different configurations of the tricycle is now compared for statistically significant differences for all three metrics. The one-way ANOVA shows no significant change in the maximum yaw factor across the four configurations, $F(3, 21) = 0.51$, $p = 0.677$ The score of the maximum yaw factor improves for 25% tie rod angle, to start decreasing for larger tie rod angles. The increased performance during this second configuration is in line with the observations. With 75% tie rod angle, the performance has decreased which is as expected. As the rider performed the manoeuvre with this vehicle very slowly and hit the tilt limit, this is an extra disadvantage. The vehicle was found to be almost unsteerable with riding when the tie rods are in this configuration.

The one-way repeated measures ANOVA shows a significant change in the mean absolute steer angle during the low-speed line-following for the four configurations, $F(3, 31) = 64.65$, $p < 0.001$. This proves that by increasing the tie rod angle, the vehicle can track the line better, which shows more balance. The post-hoc paired t-tests test using a Bonferroni corrected $\alpha = 0.05$ indicated that all changes in pairwise configurations show a significant effect, except between tie rod angles of 50% and 75%.

The one-way repeated measures ANOVA shows a significant change in the average time delay between the roll rate and the steer rate for the three configurations that could obtain a score, $F(2, 26) = 9.94$, $p = 0.002$. This means that by increasing the tie rod angles, the vehicle becomes more responsive. The post-hoc test shows significance for changes between 0% and 50% tie rod angles and between 25% and 50% tie rod angles.

5.4. Discussion

The goal of the design of the tricycle was to behave as close to the equivalent bicycle as possible in the configuration with a 0% tie rod angle. This has not been completed perfectly as the t-test shows a significantly decreased performance in the test.

By changing the tie rod angles to 25%, the controllability of the steering during the slalom, the low-speed mean absolute steer angle and the time delay all improve. By increasing the tie rod angles further, the low-speed balance keeps improving and the performance during the slalom starts decreasing again. Each time the tie rod angles are increased, the scores on the mean absolute steer angle and the average time delay between roll rate and steer rate improve. This indicates that it has been proven that the vehicle can track a line better with more balance and that the responsiveness increases by increasing the tie rod angle.

The results have shown that the configuration with the optimal handling performance is the third configuration with a tie rod angle of 50%. The normalization scale shows that the performance of the configuration (TT3) is far better and visualized more to the right than conventional bicycles, which may seem counterintuitive. This result has been obtained because the low-speed performance contributes as much to the total score as the moderate-speed performance, which readings may find less important. This low-speed performance has increased significantly.

Between configurations with tie rod angles from 0% to 50%, the maximum yaw factor shows no significant change in performance. The time to complete the slalom is also similar between these configurations which is therefore in line with the obtained data. Therefore, it can be concluded that during the slalom, the handling performance has not decreased significantly for tie rod angles between 0% and 50%.

In the slalom manoeuvre, statistically significantly decreased performance was expected for large tie rod angles. The score for 75% tie rod angle can show less decreased handling performance than expected due to the negative bias and the relation between the yaw factor and velocity, as explained in the previous section. Because of this, the time to complete the manoeuvre is required as well to interpret the results. The time to complete the slalom manoeuvre shows that the slalom could only be performed very slowly for tie rod angles of 75%, which indicates a decrease in handling performance. This all indicates that the handling evaluation metric during the slalom is less suitable for comparing the configurations of the tricycle with this low-velocity limit.

The Bonferroni correction has made the post-hoc test very conservative, which increases the chance of a type-2 error, which is the chance that a significant effect is not detected [1]. In other words, it is possible that more significant effects are found when more trials are added, between the pairwise comparisons. With the effects that are found, it is possible to conclude this thesis.

However, during the trials, the tilt limit has been hit multiple times. It is important to note that during more extreme situations, the configuration might offer too little tilting. This means that it is safer to select the third configuration if the tilt limit is increased and more extreme manoeuvres can be performed on the vehicle in a safe way. The second and third configurations offer an increase in low-speed balance that will help a healthy rider to stay upright during low speeds. This means that in conclusion, it is a good fit for commuter vehicles in city traffic to fix the vehicle in the second configuration, or in the third configuration if the tilt limit is increased. Chapter 6 will perform an optimization study to increase this tilt limit such that the third configuration can be used as the optimal configuration. With increased tilt capacity, the vehicle can safely be fixed in this configuration. For everyday city traffic for a commuter vehicle, this configuration should be used as a standard with fixed tie rod angles.

A continuous variable mechanism could be applied, to exploit the benefits of the increased low-speed performance. More sportive usages can require faster rolling and increased tilt limit. As the performance at higher speeds decreases for larger tie rod angles, and the balance is already improved in the third configuration, it is recommended that the fourth and fifth configurations are not used in the mechanism. Next to the decreased performance, unsafe maneuverability has been observed where the vehicle is also close to capsizing for tie rod angles of 75%. This means that it is sufficient to let the range of the tie rods vary between 0% and 50% for the best performance. This decreases the range that the variable mechanism should be able to move the tie rods. This can make the mechanism easier to manufacture.

Additionally, the electrical mechanism can change the tie rods to 100% when coming to a stop to fix the tilting at traffic lights. Older riders and people with physical limitations could benefit from this fixed stiffness. If this is implemented, the full range needs to be included again in the mechanism. Another

type of tilt lock can also be concidered to keep using only the range between 0% and 50%. While riding, it is hardly possible to fall while using a configuration with tie rod angles between 25% and 50%.

Because of limited time, it is not possible to test more different tie rod angles. It is possible that tie rod angles slightly above 50% shows good performance as well, but a fixed tie rod angle of 50% shows the optimal result of all tie rod angles that could be tested.

6

Chapter 6: Tilt limit optimization

Now that the configuration has been determined with the best handling performance, it is also valuable to optimize the tilt mechanism for a larger tilt limit to make the vehicle safer, to be able to answer the last subquestion of this thesis.

When the vehicle hits the limits of the tilt mechanism, unsafe situations can occur. This happens for instance during the slalom with a 50% tie rod angle. The handling performance is evaluated in specific manoeuvres, but the vehicle can be exposed to more extreme manoeuvres where the limits of the vehicle are tested more than in the test manoeuvres. Therefore, in addition to a high score on the handling tests, the tilt limit of the vehicle should be as large as possible. In other words, the optimal design of the parts of the tilt mechanism is investigated for as much tilt capacity as possible. Before the optimization method can be introduced, it is important to know the selected domain of optimization. The following method can be used to optimize the parameters of every narrow tilting vehicle, but this study will optimize the front assembly of the Dressel vehicle.

6.1. Method

This optimization study focuses on the optimization of the front assembly, where not all parameters are picked to optimize. For instance, the frame height is kept constant and also the parameters of the wheels are not changed. The parameters of the A-arm are assumed to be standard and are not investigated in this analysis as well.

The prototype of the Dressel vehicle also includes Ackermann steering, to reduce tire scrub on the ground. This means that the inner wheel has a different turning radius than the outer wheel, to realize a perfect rotation about a shared center of rotation [25]. The parameters of the steering components that have led to correct Ackermann steering will not be investigated.

This study optimizes the front assembly of the narrow tilting vehicle by investigating three variables:

1. The bell crank width (BCW).
2. The bell crank offset vertically from the pivot point of rotation (BCO).
3. The tie rod angles (TRA).

A Matlab model made by Dressel, the designer of the Dressel tilting tricycle, is used to model all possible designs of the front assembly of the vehicle. The additional function has been implemented to shift the bell crank upwards and downwards while rotating around the original pivot point. Now the three variables can all be altered and the model can compute a sweep over all possible steer and tilt angles with the selected configuration. For this optimization, the model is only swept over all combinations of tilt angles and tie rod angles. The simplified geometry of the tilting tricycle can be seen in figure 6.1. The bell crank is shown in black, the vertical green bars indicate the tie rods that connect the blue A-arms to the bell crank.

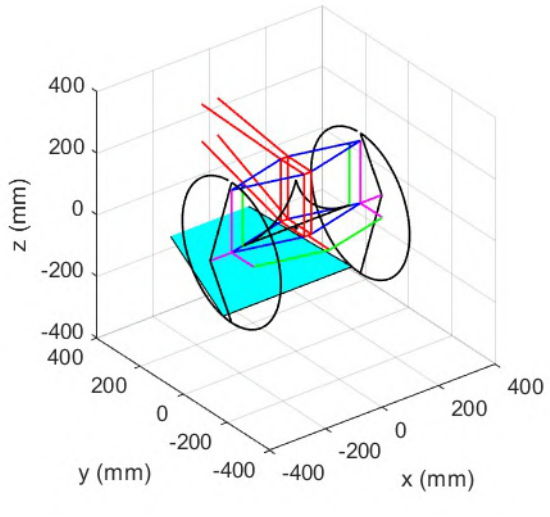

Figure 6.1: The simplified geometry of the tilting tricycle in the Matlab model made by Dressel.

6.1.1. Objective function

As stated above, the goal of this optimization study is to optimize the maximum tilt angle of the vehicle. The objective function is dependent on three variables and can therefore be written in the form of $f(x, y, z)$. This leads to a four-dimensional optimization study. It is desired to keep the optimization intuitive and visualization is important. As the 4D sweeps demand more computational effort, it has been chosen to investigate five tie rod angles and optimize for the bell-crank width and offset for each of these five important tie rod angles. In the physical experiments with the Dressel vehicle, the configurations do not fully align with the tie rod angles in the optimization but it is still possible to obtain information from this study. This leads to a simplified optimization study where the objective function is evaluated in five 3D cases. The objective function can now be written in the form of $f(x, y)@z$. The results from this optimization can be used to change the dimensions of the bell crank now that it has been determined that optimal handling is found in configuration three with a tie rod angle of 50%.

The following subsection will explain which five tie rod angles are examined.

Tie rod angle evaluations

The tie rods have a range from fully outward, where the rods are aligned parallel, up to rotated tie rods up to an angle of 35 degrees. With a default width of the bell crank, the ends of the tie rods now touch like a triangle in the simplified model. This will lead to a rigid vehicle. With tie rod angles of 0%, the trajectory of the seat of the vehicle will fall, around a circular arc. When the tie rods are pointing more inwards, the maximum tilt angles are limited but also the seat will fall with a less steep curve. The trajectory of the center of the vehicle can also rise. Now seat rise occurs. Under a specific angle, the tie rods can lead to a situation where the seat does not fall nor rise, and neutral stability occurs. In this configuration, all lateral forces are balanced and it is not possible to ride the vehicle and steer the vehicle at the same time, because the lateral forces are canceled out. This has also been recreated in the study of Dong et al., (2014) with the use of springs in the Bricycle, and Pierson et al., (2020) with another tilting tricycle with variable geometry [13, 32]. This situation is also investigated as this behaviour can have specific advantages.

This optimization study is performed over the following five tie rod angles to optimize for all bell crank widths and offsets:

1. Tie rods placed 0%.
2. Tie rods placed 20%.
3. Tie rods placed for neutral stability.
4. Tie rods placed 60%.
5. Tie rods placed 80%.

The exact angles of the tie rods where the behaviour of neutral stability starts to occur are dependent on the bell crank width and offset. For instance, neutral stability occurs at a lower tie rod angle if the bell crank has a positive vertical offset.

The next goal is to obtain the expression for the five objective functions for the maximal tilt angle of each tie rod angle evaluation. It has been investigated if an analytical relation could be found between the resulting tilt angles based on the variables of the geometry of the vehicle, but with the number of bodies of the vehicle, this is very complex and not convenient.

To obtain the objective functions, the tilt angles are obtained from the simulation. When the simulation has swept for every combination of tie rod angle, bell crank width, and bell crank offset, the maximum tilt angles can be extracted. With a large set of data points, a sufficiently accurate relation can be created between the tilt angles and the variables by the use of polynomial curve fitting. The polynomial with its characteristic coefficients is therefore the objective function that is optimized.

Curve fitting

All data points are copied to a data frame and the tilt angles have been extracted. The Matlab Curve fitting toolbox has been used to fit a polynomial of order n, m to match the data points with a selected accuracy. The order of the polynomial is decreased to an order that is as low as possible while still finding a correlation with the data points of at least a correlation coefficient $R^2 = 0.98$. According to Taylor (1990), a very high correlation is obtained from correlation coefficients $R^2 > 0.9$, and therefore the selected minimum correlation of 0.98 is high [37]. Because there is no noise in the measured data points, and the lowest order of the polynomial is selected that is possible, the risk of overfitting is reduced.

Figure 6.2 shows the result of the curve fitting toolbox for the data set where the tie rod angles are 0 degrees. The other four curve-fitting results can be found in Appendix B.

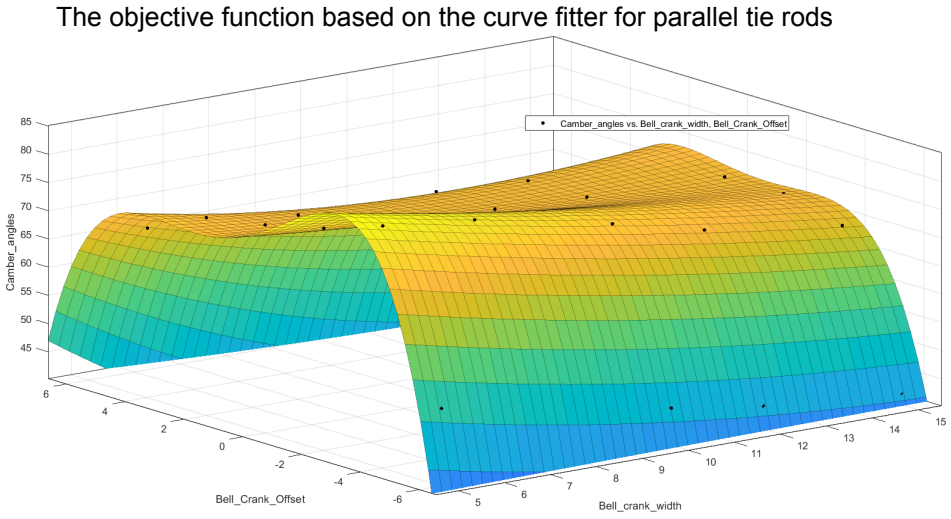

Figure 6.2: Curve fitting results of the objective function with tie rod angle = 0. $R^2 = 0.98$. The x-axis shows the bell crank width, the y-axis shows the bell crank offset and the z-axis shows the maximum tilt angles obtained from the sweep of the Matlab model.

This polynomial has order $n, m = 2, 4$. The objective function is now obtained in the following form:

$$\begin{aligned} f(Bco, Bcw) =& C_{00} + C_{10}Bcw + C_{0,1}Bco + C_{1,1}BcwBco + C_{2,0}Bcw^2 \\ &...C_{n,0}Bcw^n + C_{0,m}Bco^m + C_{n,m}Bcw^nBwo^m \end{aligned} \tag{6.1}$$

With the coefficients reported in table 6.1;

Table 6.1: The coefficients of the objective function for the maximum tilt angles with parallel tie rods.

Coefficient	Value [-]
C00	80.63
C10	-1.286
C01	-2.824
C20	0.042
C11	0.048
C02	1.068
C21	0.010
C12	-0.087
C03	0.121
C22	0.002
C13	-0.010
C04	-0.035

6.1.2. Constraints

As the problem requires constrained nonlinear optimization, the constraints need to be set up before the algorithm can start finding the optimal solution of the objective function. Impossible designs need to be excluded. A set of constraints can consist of linear and nonlinear constraint equations. This section will elaborate on the derivation of the constraints.

Boundary equations

The first constraints of the optimization problem are the linear boundaries, or limits, of the design variables.

The bell crank width, the bell crank offset, and the tie rod angles all have minimal and maximal dimensions that can be used in a viable design.

The bell crank needs to be manufactured with precision and strength. Also, the tie rods need to be able to be connected to the bell crank and enough space needs to remain for tools that can fix the rods in place. Therefore, a minimum width of 100 mm has been chosen after configurations. To determine the maximum width of the bell crank, the model of the vehicle needs to be inspected. Under no single tilt angle, the bell crank must collide with the frame or with one of the wheels. To prevent this, the bell crank can have a maximum width of 380 mm.

The bell crank offset also has finite extremes. Because the bell crank should not be able to collide with the ground, the maximum negative offset can be -65 mm. Because the bell crank should not be able to collide with the top of the front frame as well, the maximum positive offset can be +65 mm. An important aspect to note is that a bell crank with a vertical offset will still rotate around the original pivot point at the center of the frame that corresponds to the neutral position.

The minimum tie rod angle is trivial, zero degrees. The model will automatically place the tie rods parallel independently of the bell crank width. This means that the connection point of the tie rods to the A-arms can move with the bell crank width. The boundaries of the design variables are summarized below.

$$100 < BCW < 380[mm] \tag{6.2}$$

$$-65 < BCO < 65[mm] \tag{6.3}$$

$$0 < TRA < 35[^\circ] \tag{6.4}$$

Linear inequality constraints

Next to the boundary equations, more linear constraints need to be added to the optimization problem to be able to accurately solve the optimal configuration without being able to reach unviable results.

As stated before, the bell crank offset has a maximum for when it will collide with the top frame. However, for wider bell cranks, this maximum offset lowers as the top of the bell crank can collide with the frame of the tricycle sooner if the bell crank itself is also higher.

A linear relationship has been found between the maximum bell crank height, which is directly related to the bell crank width, and the maximum bell crank offset. this has led to the following linear equation that can be added to the set of constraints:

$$BCO < 6.824 - 0.435BCW \tag{6.5}$$

This equation has been determined by running the model over a sweep of selected parameters and calculating the collision point.

Nonlinear inequality constraints

In addition, nonlinear constraints exist next to the linear constraints. As shown in the middle subfigure of figure 6.3, it is desired that the change in tie rod angles change the trajectory of the seat from a falling trajectory, into a flat line, into a rising trajectory. This ensures that the falling trajectory of the seat is the most equivalent to the corresponding bicycle when the tie rods are parallel and does not fall more. If so, the neutral stability occurs around the halfway point of moving the tie rods inwards. However, it has been observed that for combinations of bell crank widths and offsets, this behaviour does not exist anymore. For too low and narrow bell cranks, the seat falls only harder when the tie rods are moved inwards. For too high and wide bell cranks, the seat rises only harder when the tie rods are moved inwards. This is shown in the top and bottom subfigure of figure 6.3

By careful analysis of the data with a sweep of data points, the limits of this behaviour are found and data points are used in a 2D regression analysis that is able to create the equation for the nonlinear constraint with a correlation coefficient of 0.94.

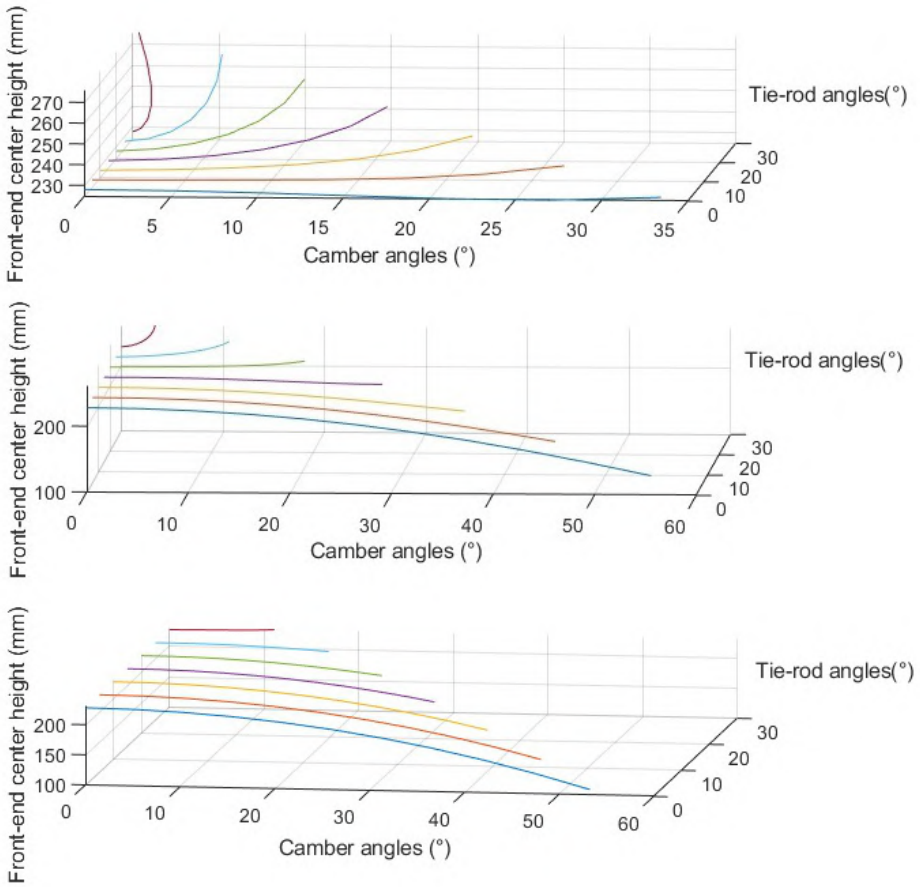

Figure 6.3: The trajectory of the seat while tilting, for different tie rod angles. The top and bottom subfigure show invalid behaviour that is observed for different combinations of bell crank widths and offsets. The constraint limits the behaviour of the seat fall to the middle subfigure.

The two resulting nonlinear constraints are:

$$BCO > 0.568 + 0.253BCW - 0.0065BCW^2 \tag{6.6}$$

$$BCO < 0.47 - 0.243BCW + 0.00634BCW^2 \tag{6.7}$$

6.1.3. Optimization algorithm

The inequality constraints and the objective function are loaded into Matlab by creating a function that returns the tilt angle at the configurations. Now, the Matlab nonlinear optimization algorithm fmincon() is used.

This algorithm makes use of the Quasi-Newton method. This method calculates local minima and maxima by computing where the gradient G of the objective function is zero, while saving computation time compared to Newton's method.

6.2. Results

After all objective functions, boundary conditions, and constraint equations have been set up, the optimization algorithm can start to find the optimal configuration while satisfying the constraints.

6.2.1. Contour plots

The design problem can be visualized best using contour plots. The 3D design problem is displayed on a flat surface and the constraints are added. This way, course optimization can take place through an investigation by eye. Figure 6.4 shows the contour plot of the objective function where the tie rods are placed parallel.

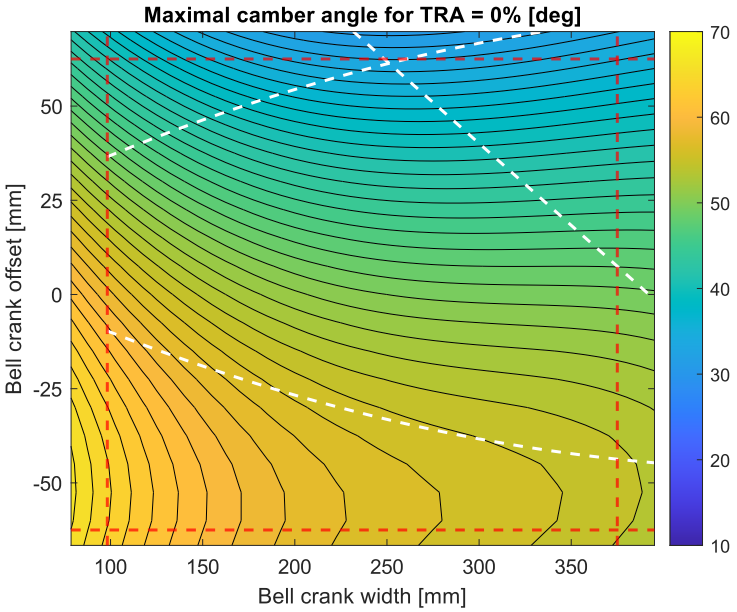

Figure 6.4: The contour plot of the objective function with the boundary conditions in red, the linear and the nonlinear constraints in white.

This figure can be used to see that for parallel tie rods, the rough estimate of the design with the largest maximum tilt angle is a design with tie rod angles of zero, a bell crank width of 100 mm, and a bell crank offset of roughly -8 mm. According to the contour plot, this maximum tilt angle is around 60 degrees. The algorithm will determine the precise optimal configuration. These results are reported in the next subsection.

In the same way, this can be done for all four other tie rod angle evaluations.

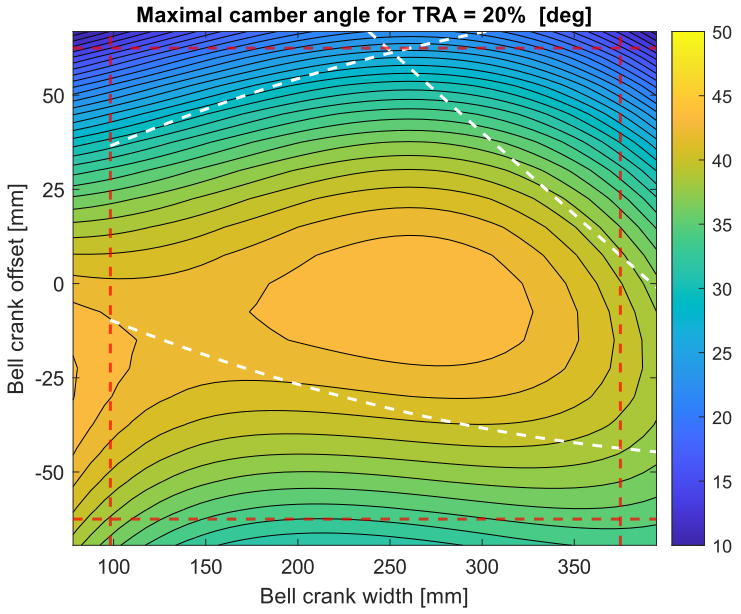

Figure 6.5: The contour plot of the objective function with the boundary conditions in red, the linear and the nonlinear constraints in white.

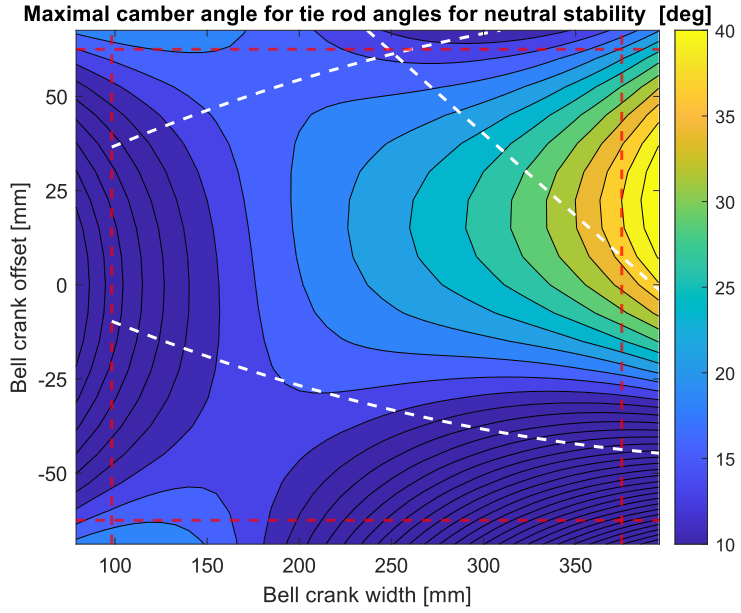

Figure 6.6: The contour plot of the objective function with the boundary conditions in red, the linear and the nonlinear constraints in white.

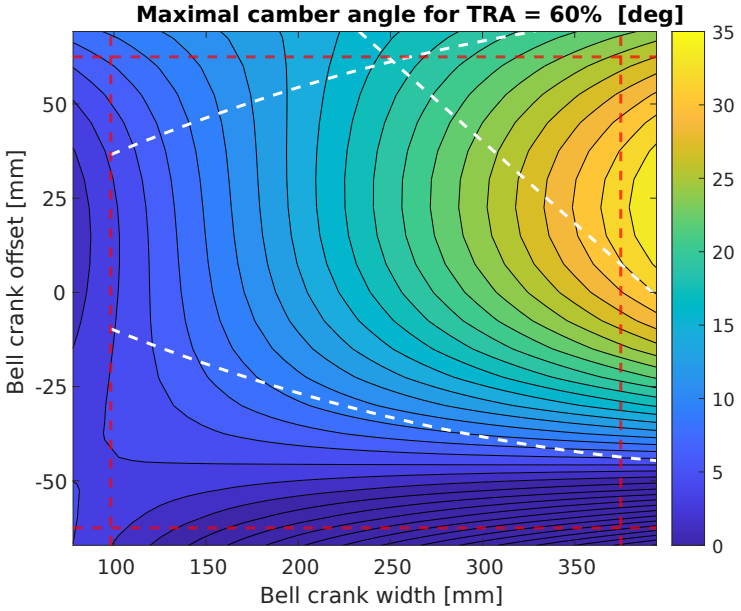

Figure 6.7: The contour plot of the objective function with the boundary conditions in red, the linear and the nonlinear constraints in white.

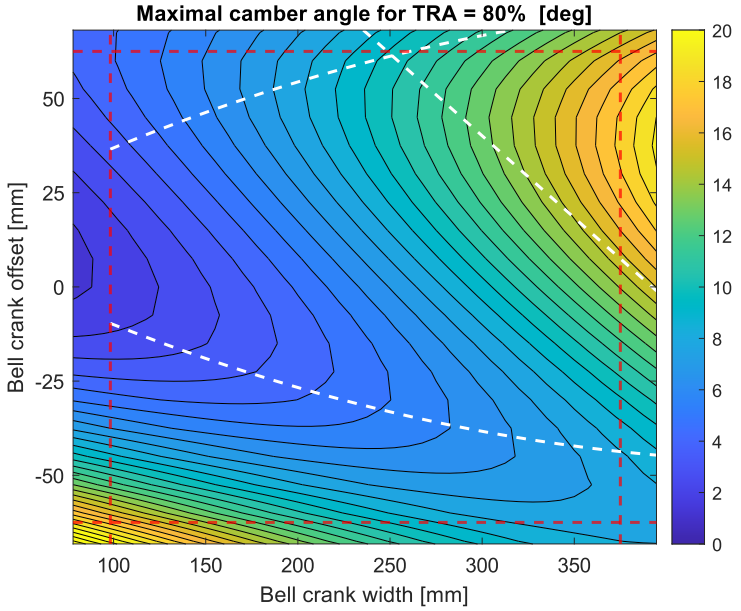

Figure 6.8: The contour plot of the objective function with the boundary conditions in red, the linear and the nonlinear constraints in white.

The contour plots already give insight into the design of the tricycle with the maximum tilt angle. As mentioned before, a lowered and narrow bell crank is desired for parallel tie rods. With the tie rods shifted inwards, the optimal configuration consists of the bell crank that is as wide as possible and placed as high as possible while satisfying the constraints.

It can be observed that for four out of the five evaluated tie rod angles, the optimal design is at the intersection of constraints and boundaries. This means that it is important to satisfy these constraints, as otherwise a configuration would be selected which would cause problems in the manufacturing, or would cause collisions in the system.

Although it might be implemented to be able to change the tie rod angle while riding, it is currently not possible to change the bell crank width and offset while riding. Therefore, a fixed width and offset should be selected. From the handling tests, tie rod angles of 50% have been shown to result in optimal handling. Therefore, the bell crank width and offset can be selected for tie rod angles around this optimum.

6.2.2. Optimal design

The algorithm will determine the more precise designs for maximal tilt and this corresponds accurately with the rough observations from the contour plot. The optimal designs for each of the tie rod angles are stated below in table 6.2. As described before, the bell crank width and offset need to be selected for the configuration that will be used most by the riders.

Table 6.2: The resulting configurations for optimal tilt limits for the five tie rod angles.

TRA	Max. Tilt angle [°]	Configuration
TRA = 0%	61.31	BCW = 100 mm BCO = -82 mm
TRA = 20%	44.33	BCW = 297 mm BCO = 2 mm
Neutral stability	36.89	BCW = 380 mm BCO = 7.6 mm TRA = 51%
TRA = 60%	31.43	BCW = 380 mm BCO = 7.6 mm
TRA = 80%	15.28	BCW = 380 mm BCO = 7.6 mm

The tie rod angles in the Matlab optimization do not align with the tested tie rod angles in the physical experiments with the Dressel vehicle. In future research, more tie rod angles could be tested physically. However, the experiments showed that tie rod angles of 50% have the best handling, but the tilt limit is reached. Therefore it is important to apply this optimization to redesign the tilt mechanism for larger tilt limits. Table 6.2 shows that for tie rod angles between 50% and 60%, the bell crank should be 380 mm wide and that the bell crank should be moved roughly 7 mm upwards up to a height of 235 mm.

By running the simulation with the realized dimensions of the bell crank, the theoretical tilt angles of the tricycle can be reported, table 6.3.

Table 6.3: The maximum tilt angles obtained by running the simulation with BCW = 290 mm and BCO = 0 mm.

TRA [%]	Max. Tilt angle [°]
0%	55
20%	36
Neutral stability	22
60%	15
80%	8

From the table, it can be concluded that the maximum tilt angles can be increased. For a tie rod angle of 50%, it can be extracted from the simulation that 15°degrees of extra tilt capacity can be added. This makes the vehicle safer and more suitable for turns at higher speeds.

The maximum realized tilt angles for all tie rod angles of the realized prototype can be found in table 6.4. The realized tilt angles are significantly lower than the maximum tilt angles that are theoretically achievable. To be able to manufacture the tricycle, DEMO made design choices that lead to collisions that reduce the maximum tilt angle. The tie rod angles were found to hit the connection rod that the manufacturer included to fix the tie rods to the bell crank. To be able to use the maximized tilt limits, the shape of the connection rod should be altered too, or the tie rods should be fixed to the bell crank after which the connection rod can be removed.

Table 6.4: The realized maximum tilt angles for each configuration of the physical prototype of the Dressel tilting tricycle with BCW = 290 mm and BCO = 0 mm.

TRA [%]	Max. Tilt angle [°]
0%	33
25%	24
50%	13
75%	6
100%	1

If a mechanism would be added that can alter the tie rod angles, the optimal bell crank width and offset changes according to the results. Therefore, this is not beneficial for the optimal tilt limits. The bell crank width and offset should be selected with the tie rod angles that will be used during the largest share of the time as a compromise.

6.3. Discussion

The results from the simulation show that neutral stability occurs around TRA = 51%, with the dimension of the realized bell crank. The physical prototype shows that the trajectory stays on a straight line around 70%, therefore the simulation does not match the physical prototype perfectly. Also, the realized tie rod angle is larger than 35°degrees. This is the case because of small changes in the design that have made the manufacturing possible. As mentioned before, the maximized tilt angle can only be used when the connection rod is redesigned.

In the configuration closest to the neutral stability (TRA = 75%), the handling tests show problems with steering the vehicle while riding, with comparable behaviour to the previous studies [13, 32]. This behaviour can result in dangerous situations as the rider cannot turn the vehicle and it is not recommended to include this configuration into the range of possible tie rod angles when a variable mechanism would be implemented. This is an additional argument to fix the tie rods at 50%.

The non-linear constraints keep the neutral stability possible to achieve with a specific tie rod angle. This study has not found any practical benefits or applications of this setting, but future research might benefit from this behaviour in a different application. Dong et al., (2014) state that there might be applications for learning to ride a bicycle [13]. If future research points out that there is no specific application for neutral stability, the lower bound of the non-linear constraint can be removed from this optimization study.

7

Chapter 7: Discussion

The goal of this thesis was to optimize the tilt mechanism of the Dressel tilting tricycle for optimal handling performance for a commuter vehicle in city traffic. The findings of this study provide important insights into how the handling performance can be measured and into the performance of the Dressel tilting tricycle itself. In this chapter, I discuss and interpret the combined results that have been obtained from the research and experiments. The obtained results are compared with the findings in the literature. Furthermore, the implications of the findings and the areas for future research are analyzed.

7.1. Handling evaluation method

In this study, I created a method to evaluate a large range of handling performance of a vehicle. The metrics have been selected and the tests have been designed for the most representative scores for commuter vehicles in city traffic. The results show that city traffic vehicles lead to higher scores in the handling tests. A more sportive model leads to a decreased score. This shows that the handling evaluation method is capable of scoring the performance for good and comfortable handling for commuting.

Not all differences in the performance of the bicycles can be traced back to the trail, wheelbase, and head angle. The other design parameters contribute to different handling performances as well, but these effects have not been analyzed during this study.

The results of this study show that the average time delay between the roll rate and steer rate varies between 160 milliseconds for the least responsive bicycle and only 46 milliseconds for the best configuration of the Dressel tricycle. This can make a strong difference in situations where quick responses are required, such as for obstacle avoidance. For bicycles, Kovacsova et al., (2016) report similar time delays between 120 and 160 milliseconds [22]. The obtained time delay of Cain (2012,2016) is also in the same order of magnitude [5, 6]. For the mean absolute steer angle, the authors show results between 2.5 and 3 degrees. Higher mean absolute steer angles have been reported for regular bicycles in this study. However, the speed during their manoeuvre is higher, which makes the low-speed line-following easier [22]. By changing vehicles to a tricycle with the optimal tilt mechanism, the mean absolute steer angle could be decreased to 2.3 degrees at a more difficult speed. Zellner and Weir (1978) show linear and curved relationships between the yaw factor and the forward velocity, dependent on the model of the vehicle [41]. A similar relation has also been found in this study, although the exact shape cannot be determined due to variability in performance between the trials. For speeds that are typical for bicycles, similar values for the yaw factor have been obtained that need to be minimized for an optimal steer characteristic.

The three metrics have been shown to be able to distinguish performance between vehicles. However, limitations of the method have been found. When the design of two vehicles is almost identical, the number of trials has led to a standard deviation which has made it unable to conclude on a significant level anymore. This means that when comparing two closely related designs, as many trials as possible should be added. The average time delay between the roll rate and steer rate was found to be limited to vehicles with roll freedom, as the coupled correlation of the two angular velocities is not present

anymore for a 75% tie rod angle. The maximum yaw factor can be scaled for lower velocities, but the results become less accurate if the velocity difference is large and the vehicle is physically not able to complete the manoeuvre at the desired speed. This means that the metric is most useful for comparing vehicles with similar speed limits. Therefore, it was required to use the time to complete the manoeuvre as additional information.

The selection of the metrics was limited to metrics that use kinematic data, as no data on the torque on the handlebars could be obtained. A torque sensor attached to the head tube or a force sensor on the handles could be added in future research to provide even more information on the handling performance. More opportunities for different handling metrics will then open. This was found to be not reachable in the time span of this study.

Scores of different designs of the tilting tricycle have shown to be able to transcend the scores of regular bicycles. This is mainly the case because low-speed line-following performance could be improved, while not sacrificing the performance at higher speeds. As mentioned before, the scale factors for combining the metrics into a single score can be changed if researchers want to emphasize the performance at a higher speed.

7.2. Equipment

The kinematic data of the angular velocities have been measured with the gyroscope of the Shimmer3 IMUs in this thesis. Accurate results have been obtained after processing of the data. These canned sensors are recommended for bicycle-related studies to measure the kinematic data while riding in the simplest way.

Additionally, the velocity has been measured using the Strava GPS application. The data was used to make the trials as similar as possible between themselves by discarding trials with the wrong velocity. The sampling frequency of 1 Hz was small enough for this purpose. A real-time correction of the data based on the velocity requires a higher sampling rate. A delay in the current speed on the display has led to an overshoot in velocity.

7.3. Optimal design

This research has shown that a single configuration of the design of the tilt mechanism of the tilting tricycle results in optimal and improved handling performance. The low-speed balance and responsiveness can be improved without sacrificing performance at higher speeds. For daily city traffic usage of the commuter vehicle, it is best to fix the tie rod angles at 50% and to widen and raise the bell crank. This can make the vehicle cheaper and easier to manufacture due to the fact that the mechanism doesn't have to be variable anymore. A design with fixed tie rods can also include a tilt lock that does not make use of the variable tie rod mechanism.

However, there are still choices that the designer can make. An automatic system that changes the tie rod angles based on the velocity could make turning at higher speeds possible, as mentioned in section 5.4. The important aspect of this variable mechanism is that it should move the tie rods to 100% sharply and only when the velocity is approximately close to 0. This prevents the chance of accidentally passing through the neutral stability which might lead to accidents. Changing tie rod angles also lead to different optimal bell crank designs. The bell crank width and offset should still be selected according to the configuration with a tie rod angle of 50% as this configuration will be used the most during normal riding.

This can all make the tilting tricycle handle better and more comfortable while riding. It is assumed that the tilting tricycle offers more benefits apart from improved handling, such as increased traction and increased braking performance. This has not been investigated in this research and a new study can investigate the difference in performance of the tricycle compared to a regular bicycle in these aspects.

8

Chapter 8: Conclusion

This research aimed to identify the most suitable method to evaluate the handling performance to optimize the tilt mechanism of the Dressel tilting tricycle. The handling method has been selected to optimize the handling performance of a commuter vehicle in city traffic and combines a broad range of handling aspects. The research question of this thesis was therefore:

How can the tilt mechanism of the narrow tilting tricycle be designed for optimal handling performance for commuter vehicles?

The results of this investigation lead to the conclusion that three independent metrics can be combined into a single score for handling performance that is able to discriminate the performance between vehicles. This addresses the gap in qualitative handling evaluation methods that can decide on multiple aspects of handling. The maximum yaw factor, the mean absolute steer angle, and the average time delay between roll rate and steer rate are promising metrics for evaluating the handling performance for commuting with their respective manoeuvres. The data has been measured using only two Shimmer IMUs.

The adaptable mechanism of the Dressel tilting tricycle has been tested for four different tie rod angles. The experiments show that optimal handling performance can be obtained with a tie rod angle of 50%. Low-speed balance and the vehicle's responsiveness improve, while the moderate-speed performance at the slalom manoeuvre has not decreased significantly. Lower tie rod angles show more tilt capacity. Tie rod angles of 75% are associated with the neutral stability mode, which has led to uncontrollable behaviour at moderate speeds. Therefore, tie rod angles should not be increased further than 50%. The total score of the handling performance of this configuration has reached 0.86, compared to 0.5 for the reference bicycle.

The tilt limit of the vehicle needs to be increased for the optimal configuration to make the vehicle safer. If the bell crank is redesigned with a width of 380 mm and a height from the ground of 235 mm, the vehicle will gain more than 15°degrees of tilt capacity. The tie rod connector rod also needs to be redesigned.

The research question can be answered by the main result that a single configuration with a tie rod angle of 50% and the described bell crank dimensions has the most optimal handling performance that can be used for commuting in daily city traffic.

These findings support the hypothesis that handling performance can be improved and more comfortable riding can be created by making use of an optimal design in the tilting tricycle. These results have important implications for sustainability and also for safety. The vehicle will also reduce one-sided accidents because of its increased low-speed balance. Riders with physical limitations that struggle to keep a regular bicycle upright can benefit from the tilting tricycle. Improved handling and comfort can draw commuters onto this sustainable type of vehicle, and out of motorized vehicles for small to moderate distances. A fixed design will also make the vehicle cheaper and easier to manufacture.

Limits to the usability of the metrics arise when the vehicle becomes rigid or when the maximum velocity is substantially lower. The correlation between the roll rate and steer rate is then not present anymore. The scaling of the maximum yaw factor is more reliable for small velocity differences.

8.1. Recommendations

This research can be extended with another metric and handling test that makes use of data on the torque on the handlebars. This can give more information about the handling performance at high speeds. this score can be added to the total score using the same way of combination as described in this thesis, with another scale factor.

This study focused solely on the handling performance of the tilting tricycle, while the other benefits might be found in other aspects of the design in future research. The advantages of the tilting tricycle regarding increased traction and braking performance are yet to be investigated. Possible advantages and applications of the neutral stability mode should also be investigated.

The accuracy of the velocity measurement data can be improved when sensors with a higher sampling frequency are used. This could open possibilities to correct the data on velocity for every sample in time. Furthermore, the motion of the body of the rider is assumed to be constant between the different vehicles in this within-subject study. The differences in body motion can be investigated by making use of multiple IMUs on the body in upcoming research.

At last, the amount of trials that can be taken per vehicle is limited, and dependent on the time to analyze the data. An automatic algorithm that syncs the data of the IMUs in time by using the Unix data can save a significant amount of time which can make room for more trials per vehicle. This can improve the resolution of the handling evaluation method.

Bibliography

[1] Armstrong, R. A. (2014). When to use the Bonferroni correction. *Ophthalmic and Physiological Optics 34*, 5, 502–508.

[2] Atabani, A., Badruddin, I. A., Mekhilef, S., and Silitonga, A. S. (2011). A review on global fuel economy standards, labels and technologies in the transportation sector. *Renewable and Sustainable Energy Reviews 15*, 9, 4586–4610.

[3] Azami, H., Mohammadi, K., and Bozorgtabar, B. (2012). An improved signal segmentation using moving average and Savitzky-Golay filter.

[4] Bike dimensions. (2009). Retrieved on 01-15-2023 from `https://https://commons.wikimedia.org/wiki/File:Bike_dimensions.svg`.

[5] Cain, S. M., Ashton-Miller, J. A., and Perkins, N. C. (2016). On the skill of balancing while riding a bicycle. *PLoS one 11*, 2, e0149340.

[6] Cain, S. M., Ulrich, D. A., and Perkins, N. C. (2012). Using measured bicycle kinematics to quantify increased skill as a rider learns to ride a bicycle. In *Dynamic Systems and Control Conference*, vol. 45318, American Society of Mechanical Engineers, pp. 195–199.

[7] Chiou, J.-C., Lin, C.-Y., Chen, C.-L., and Chien, C.-P. (2009). Tilting motion control in narrow tilting vehicle using double-loop pid controller. In *2009 7th Asian Control Conference*, IEEE, pp. 913–918.

[8] Cohen, J. *(2013). Statistical power analysis for the behavioral sciences*. Academic press.

[9] Cossalter, V., Da Lio, M., Lot, R., and Fabbri, L. A general method for the evaluation of vehicle manoeuvrability with special emphasis on motorcycles. *Vehicle system dynamics 31*, 2 (1999), 113–135.

[10] Cossalter, V., and Sadauckas, J. (2006). Elaboration and quantitative assessment of manoeuvrability for motorcycle lane change. *Vehicle System Dynamics 44*, 12, 903–920.

[11] D'hondt, J., Degryse, D., Slaets, P., Demeester, E., and Juwet, M. (2022). Handling qualities of a new last-mile vehicle. *Journal of Transportation Technologies 12*, 1, 137–158.

[12] Documentation - Shimmer Wearable Sensor Technology. (2021). Retrieved on 05-20-2023 from `https://shimmersensing.com/support/wireless-sensor-networks-documentation/`.

[13] Dong, O., Graham, C., Grewal, A., Parrucci, C., and Ruina, A. (2014). The bricycle: a bicycle in zero gravity can be balanced or steered but not both. *Vehicle system dynamics 52*, 12, 1681–1694.

[14] Doyle, A. J. R. *(1987). The skill of bicycle riding.* PhD thesis, University of Sheffield.

[15] D'hondt, J., Slaets, P., Demeester, E., and Juwet, M. Effects of a torsion spring used in a flexible delta tricycle. *Applied Mechanics 3*, 3 (2022), 1040–1051.

[16] Emad-Eldin, A. A., and Öztürk, A. (1988). A modified one-sample qq plot and a test for normality. *Journal of Statistical Computation and Simulation 29*, 1, 1–15.

[17] Gazelle Ami C7 HMS (n.d.). Retrieved on 5-20-2023 from `https://www.gazelle.nl/ami-c7-hms`.

[18] Klein, R. H. *(1979). Development of Aerodynamic Disturbance Test Procedures: Technical report*, vol. 2. The Administration.

[19] Koch, J. *(1980). Experimentelle und analytische Untersuchungen des Motorrad-Fahrer-systems*. VDI-Verlag.

[20] Kooijman, J., Meijaard, J. P., Papadopoulos, J. M., Ruina, A., and Schwab, A. L. (2011). A bicycle can be self-stable without gyroscopic or caster effects. *Science 332*, 6027 (2011), 339–342.

[21] Kooijman, J., and Schwab, A. L. (2013) A review on bicycle and motorcycle rider control with a perspective on handling qualities. *Vehicle system dynamics 51*, 11, 1722–1764.

[22] Kovacsova, N., de Winter, J. C., Schwab, A. L., Christoph, M., Twisk, D., and Hagenzieker, M. (2016). Riding performance on a conventional bicycle and a pedelec in low speed exercises: Objective and subjective evaluation of middle-aged and older persons. *Transportation research part F: traffic psychology and behaviour 42*, 28–43.

[23] Meijaard, J. P., Papadopoulos, J. M., Ruina, A., and Schwab, A. L. (2007). Linearized dynamics equations for the balance and steer of a bicycle: a benchmark and review. *Proceedings of the Royal society A: mathematical, physical and engineering sciences 463*, 2084 (2007), 1955–1982.

[24] Misachi, J. (2018). America's Most Popular Ways Of Commuting To Work.

[25] Mitchell, W. C., Staniforth, A., and Scott, I. (2006). Analysis of Ackermann steering geometry. Tech. rep., SAE Technical Paper, 2006.

[26] Moore, J. (2006). Low speed bicycle stability: Effects of geometric parameters. *No publication*.

[27] Moore, J., Hubbard, M., and Hess, R. A. (2016). An optimal handling bicycle. In *Proceedings of the 2016 Bicycle and Motorcycle Dynamics Conference* (2016).

[28] Moore, J. K., and Hubbard, M. (2019). Expanded optimization for discovering optimal lateral handling bicycles. Symposium on the Dynamics and Control of Single Track Vehicles.

[29] Moritzburke, M., Toribio, A., Yang, S., and Kubicki, S. (2020). Optimal Handling Bicycle: Final Design.

[30] National household travel survey (n.d). Retrieved on 03-24-2023 from `https://nhts.ornl.gov/vehicle-trip`.

[31] Paterek, T. (2004). The paterek manual for bicycle framebuilders, henry james bicycles.

[32] Pierson, A., Shortreed, A., Van Asten, P., and Dressel, A. (2020). A narrow-track tilting tricycle with variable stability that the rider can control manually. In *International Design Engineering Technical Conferences and Computers and Information in Engineering Conference*, vol. 83938, American Society of Mechanical Engineers.

[33] Rice, R. S. Rider skill influences on motorcycle maneuvering. *SAE Transactions* (1978), 1419–1430.

[34] Rosenthal, R., Cooper, H., Hedges, L., et al. (1994). Parametric measures of effect size. *The handbook of research synthesis 621*, 2, 231–244.

[35] Schwab, A., Kooijman, J., and Meijaard, J. P. (2008). Some recent developments in bicycle dynamics and control. In *4th European Conference on Structural Control, ECSC 2008*, Russian Academy of Sciences, pp. 695–702.

[36] Schwab, A. L., Meijaard, J. P., and Papadopoulos, J. M. (2005). Benchmark results on the linearized equations of motion of an uncontrolled bicycle. *Journal of mechanical science and technology 19*, 1, 292–304.

[37] Taylor, R. (1990). Interpretation of the correlation coefficient: a basic review. *Journal of diagnostic medical sonography 6*, 1, 35–39.

[38] Tiseo, I. (2023). Global transportation sector CO2 emissions 1970-2021. `https://www.statista.com/statistics/1291615/carbon-dioxide-emissions-transport-sector-worldwide/`.

[39] Verkeersongevallen 2021 en schatting eerste helft 2022 (n.d). Retrieved on 02-06-2023 from `https://www.veiligheid.nl/kennisaanbod/cijferrapportage`.

[40] Yu, Z., Leng, B., Xiong, L., Feng, Y., and Shi, F. (2016). Direct yaw moment control for distributed drive electric vehicle handling performance improvement. *Chinese Journal of Mechanical Engineering 29*, 3, 486–497.

[41] Zellner, J. W., and Weir, D. H. (1978). Development of handling test procedures for motorcycles. *SAE Transactions*, 1431–1440.

[42] Zellner, J. W., and Weir, D. H. (1979). Moped directional dynamics and handling qualities. *SAE Transactions*, 906–919.

A

Negative trail bicycle

The negative trail of the bicycle is large, -270 mm [29]. The bicycle can be seen in figure A.1.

Figure A.1: The negative trail bicycle [29].

The large negative trail has led to uncontrollable riding. The original research on the performance of the design has shown that the real part of the stability eigenvalues is strictly negative, which indicates instability for all velocities [29]. It has not been able to ride the bicycle during the slalom manoeuvre as the steering is uncontrollable which causes dangerous situations.

The low-speed line-following manoeuvre has been performed and highly irregular behaviour is observed as steering led to roll in the flipped direction compared to a regular bicycle. No total score could be assigned to this negative trail bicycle. The negative time delay between the roll rate and steer rate with a small standard deviation shows that the handling performance evaluation method is limited to vehicles with positive trails, as the logarithmic scale cannot be used for negative scores.

To investigate the reason for this flipped time delay, the motion of the ”benchmark bicycle”, as defined by Meijaard et al., (2007), is simulated in Matlab, which is edited with a large negative trail equal to the trail of the negative trail bicycle [23]. Unstable results are found and the motion could not be simulated with the low velocities that are used during the manoeuvres. Figure A.2 shows that the controller is not able to stabilize the vehicle and that on some parts of the motion, the roll rate lags to the steer rate, as obtained from the data from the sensors. With regular bicycles, the steer rate lags to the roll rate while riding, as described before. This is also reported in previous studies [5, 6, 14, 22].

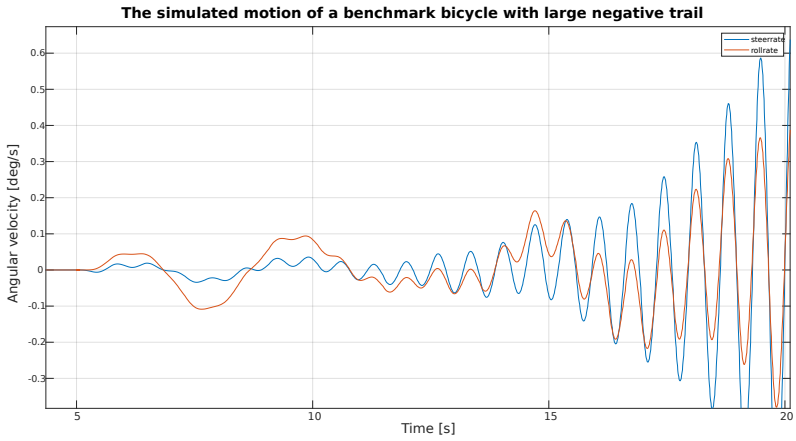

Figure A.2: The obtained motion of a benchmark bicycle with large negative trail (c=-0.27m), with a velocity of v=7 m/s. Unstable results are obtained. The benchmark bicycle is defined by Meijaard et al., (2007) [23].

However, it can not be concluded from the obtained results for the time delay with the negative trail bicycle that this behaviour is due to the geometry of the bicycle, as also other reasons such as hardware problems could have been the case. Future research can be performed to give a more precise analysis of the handling performance of the negative trail bicycle.

B

Figures

B.1. Time series

Over 360 plots would be required to show all data. Therefore, the time series of the reference bicycle are shown in figure B.1 and B.2 on the next page. It can be seen that the trials are similar.

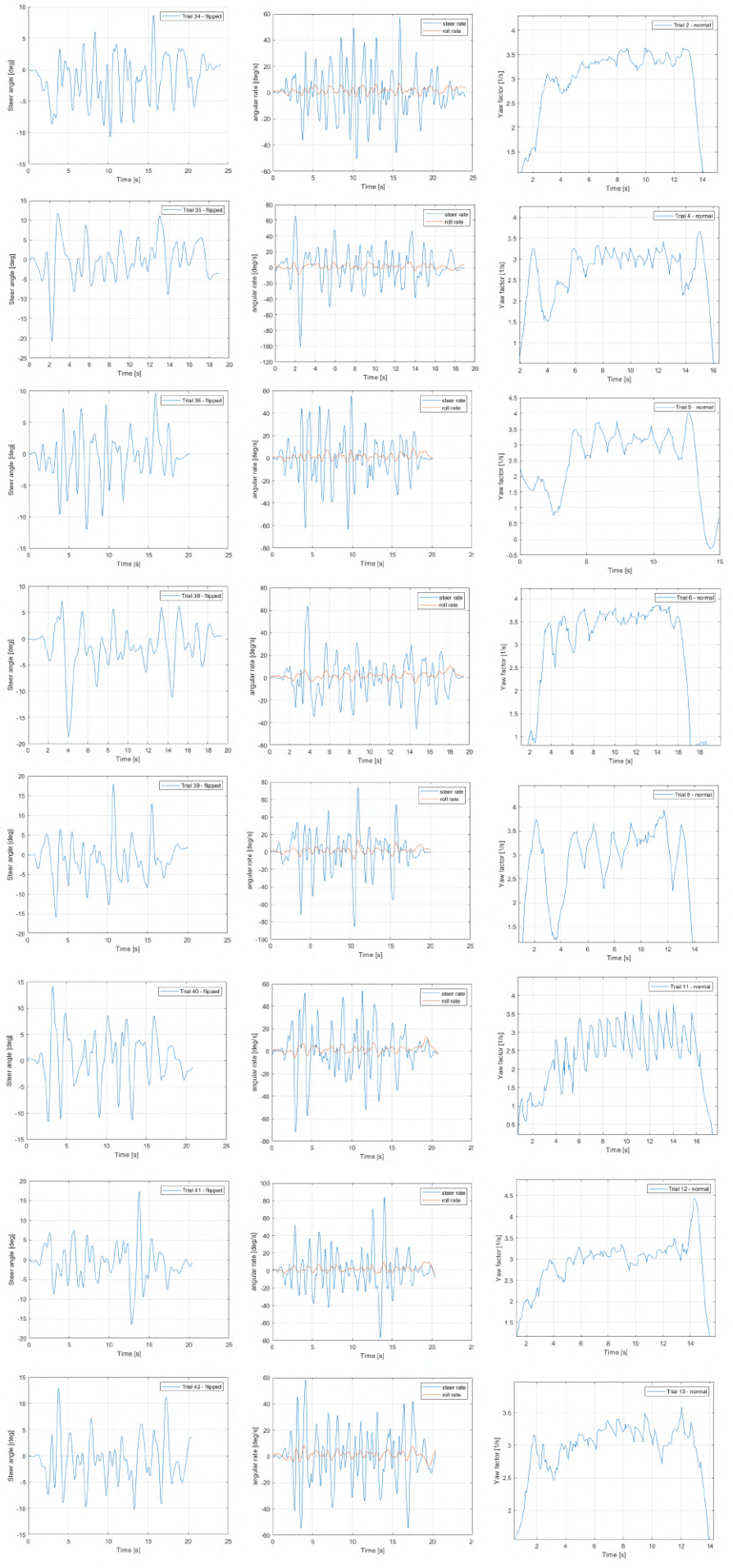

Figure B.1: The time series of the signals obtained for the reference bicycle with a normal front fork.

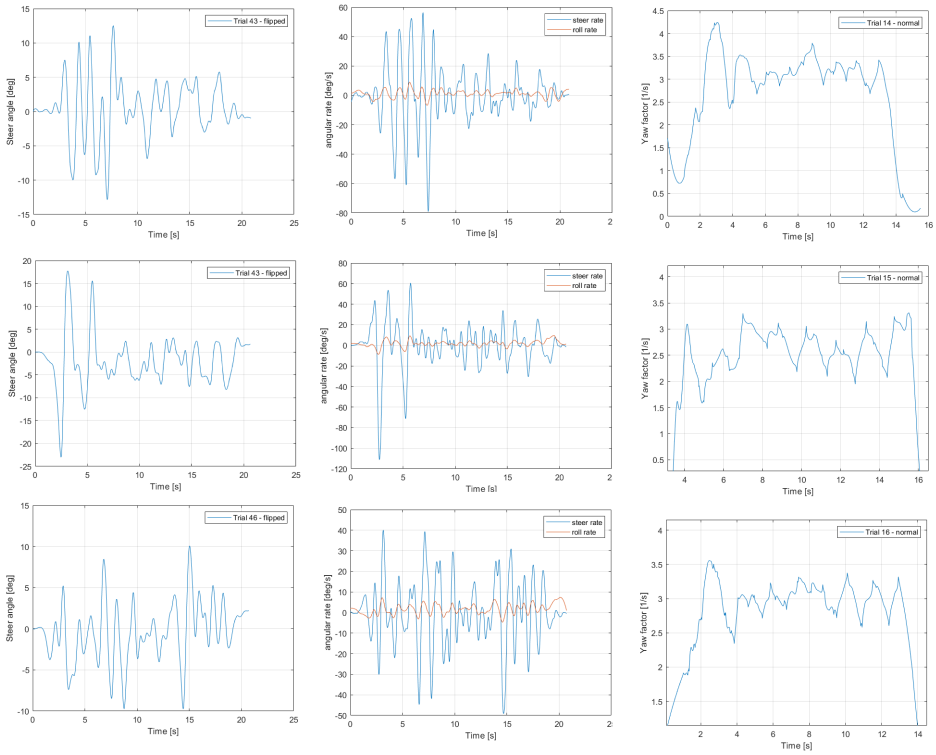

Figure B.2: The time series of the signals obtained for the reference bicycle with a normal front fork.

B.2. Curve fitting objective functions

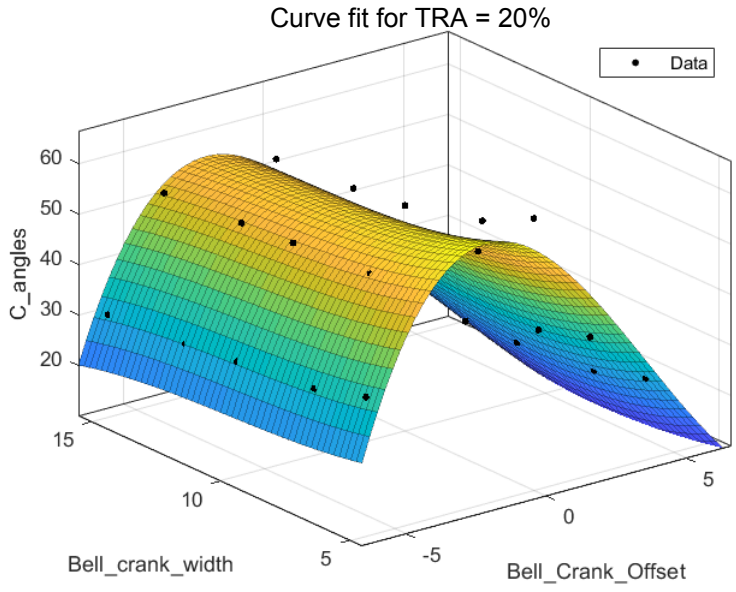

Figure B.3: Curve fitted objective function

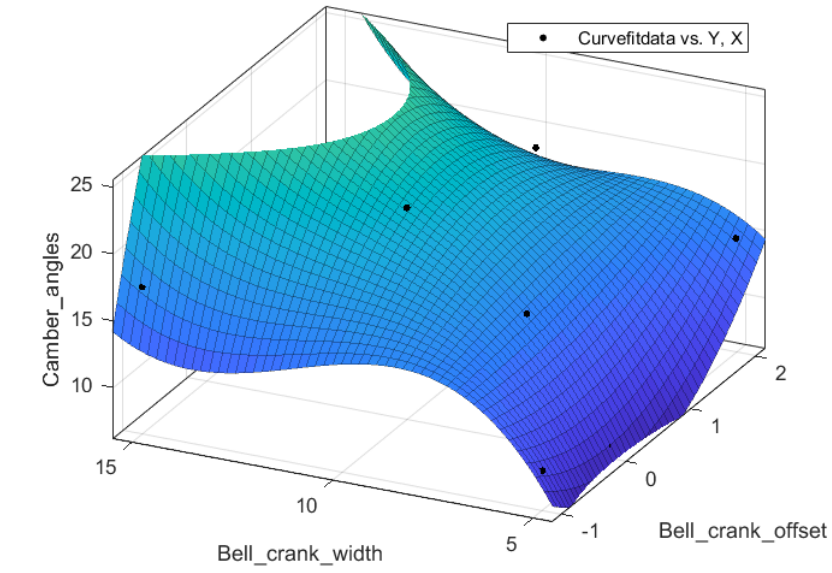

Figure B.4: Curve fitted objective function

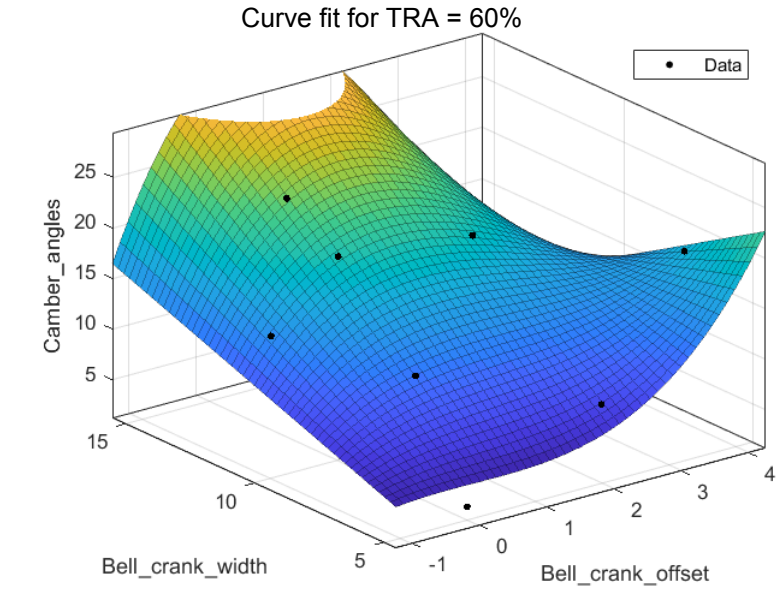

Figure B.5: Curve fitted objective function

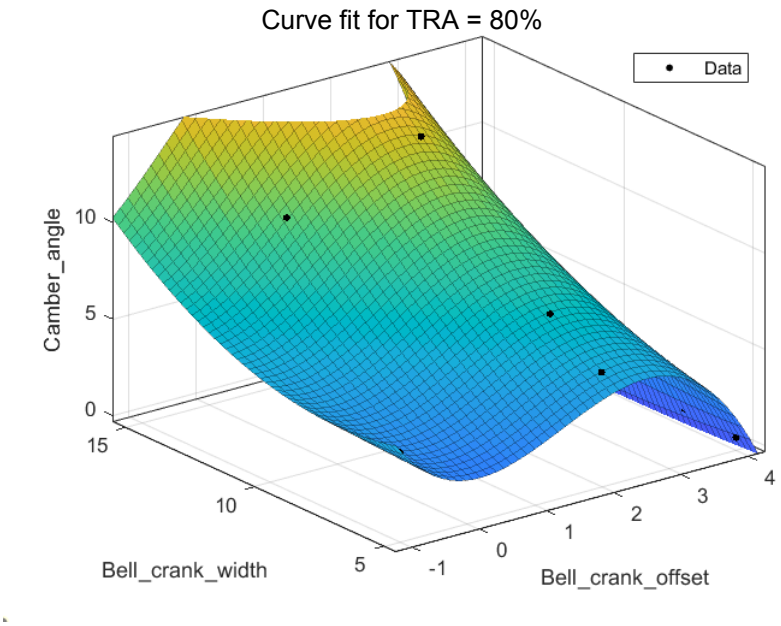

Figure B.6: Curve fitted objective function

C

Datasheets

C.1. Trial data

RESULTS OF REMAINING VALID TRIALS

Batavus straight

max yaw factor	Mean abs angle	Mean time delay	score
4.32	3.67	0.0881	
3.67	4.13	0.0915	
3.44	3.11	0.0948	
3.92	3.61	0.113	
3.43	3.54	0.117	
3.55	4.34	0.0655	
3.76	3.63	0.1134	
3.43	3.48	0.0911	
3.29	3.69	0.0798	
3.24	4.08	0.0905	
	3.01	0.107	

Batavus Flipped

max yaw factor	Mean abs angle	Mean time delay
3.87	7.06	0.215
4.04	7.65	0.186
3.86	8.47	0.165
5.55	7.41	0.14
3.99	6.75	0.163
3.96	7.49	0.147
4.35	8.07	0.165
4.28	7.85	0.153
4.55	5.77	0.137
4.08	5.57	0.131
	8.03	0.115

Gazelle

max yaw fa	Mean abs a	Mean time delay
4.06	3.6	0.18
4.05	3.5	0.111
4.31	3.43	0.0692
3.93	3.12	0.0768
4.06	4	0.0565
4.66	5.1	0.049
3.99	4.6	0.042
4.07	4.26	0.079
4.22	3.9	0.062

Giant

max yaw factor	Mean abs angle	Mean time delay	score
3.17	3.9	0.133	
4.5	4.14	0.15	
4.54	4.22	0.102	
4.47	2.17	0.127	
4.17	3.88	0.131	
4.41	3.15	0.14	
4.71	3.53	0.163	

Test trike 1 - piet

max yaw factor	Mean abs angle	Mean time delay
3.99	3.68	0.063
4.32	4.48	0.101
3.96	4.01	0.0574
3.97	3.44	0.063
4.13	3.96	0.096
4.34	3.96	0.084
4.23	2.9	0.0892
4.6	2.88	

Test trike 2 - piet

max yaw fa	Mean abs a	Mean time delay
4.83	3.53	0.089
4.94	3.3	0.131
4.86	3.06	0.067
4.92	3.98	0.13
4.7	3.64	0.067
4.84	3.59	0.057
4.87		
4.82		

TT1

max yaw factor	Mean abs angle	Mean time delay
4.68	4.03	0.069
5.08	4.14	0.102
4.92	5.32	0.094
4.79	5.5	0.048
3.81	4.68	0.101
3.87	5.5	0.064
4.31	4.44	0.144
4.23	5.23	0.117
4.39	4.29	0.134
4.51		
4.1		

TT2

max yaw factor	Mean abs angle	Mean time delay
4.39	3.26	0.0546
3.95	2.16	0.0705
4.21	3.26	0.0979
3.96	2.19	0.1064
4.58	2.42	0.0516
4.11	2.29	0.104
4.12	3.06	0.0659
4.1	2.08	0.0802
4.1	1.87	0.0672
	2.73	0.0542
	3.05	0.114

TT3

max yaw fa	Mean abs a	Mean time delay
4.69	2.73	0.0532
3.66	2.56	0.0283
5.4	2.21	0.0253
3.99	2.91	0.0512
4.38	2.13	0.0349
4.34	2.42	0.0486
3.86	1.81	0.0106
4.14	1.78	0.053
4.22	2.52	0.0592
4.11	2.39	0.0699
5.37	1.81	0.0725
4.36	2.7	0.0489

TT4

max yaw factor	Mean abs angle	Mean time delay
4.16	1.54	-10
6.08	1.52	1.86
4.15	0.75	2.76
4.02	1.3	4.04
5.14	1.03	2.13
4.25	1.24	2.58
	1.91	-0.04
	1.37	1.69

C.2. Velocity data

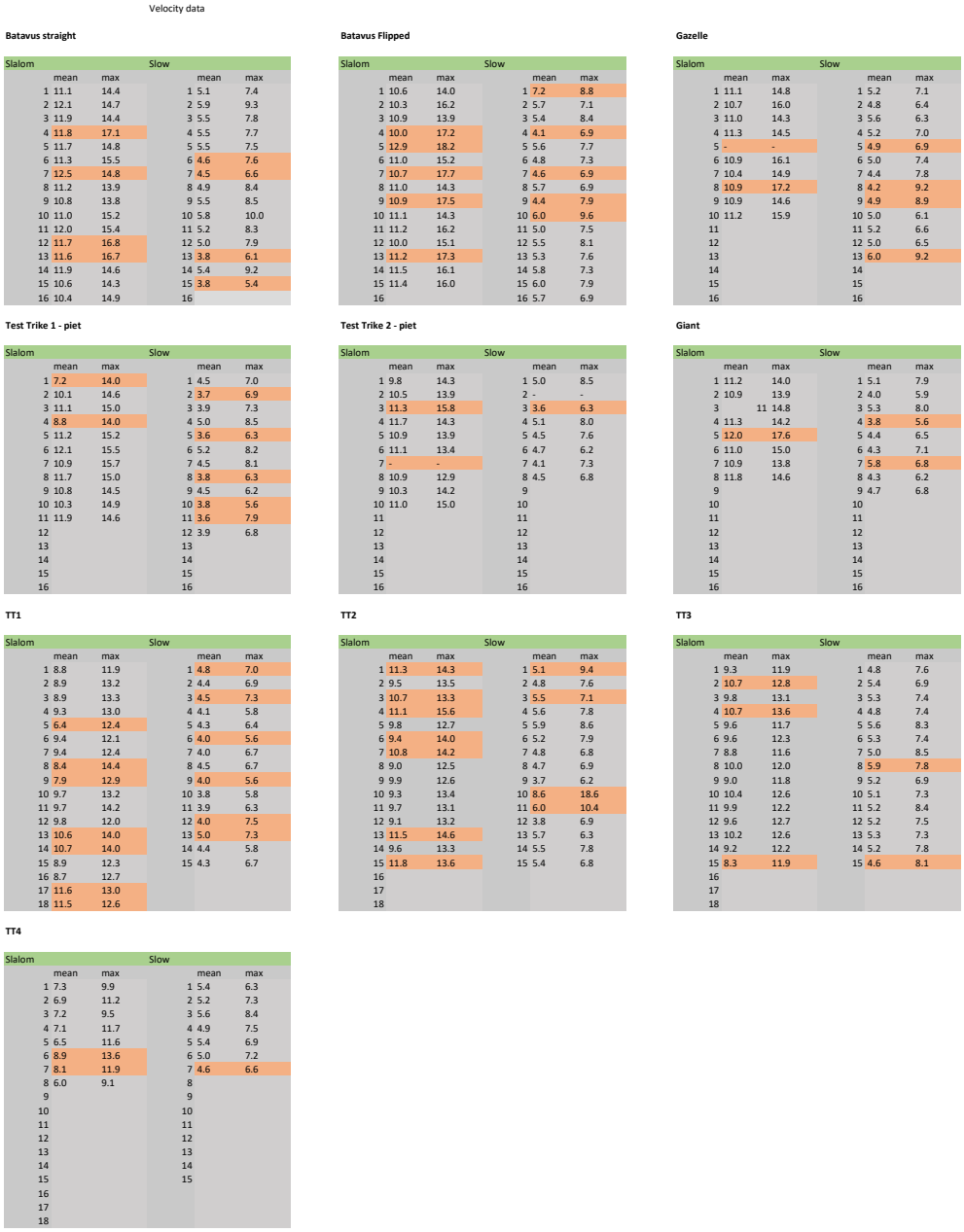

Velocity data

Batavus straight

	Slalom			Slow	
	mean	max		mean	max
1	11.1	14.4	1	5.1	7.4
2	12.1	14.7	2	5.9	9.3
3	11.9	14.4	3	5.5	7.8
4	11.8	17.1	4	5.5	7.7
5	11.7	14.8	5	5.5	7.5
6	11.3	15.5	6	4.6	7.6
7	12.5	14.8	7	4.5	6.6
8	11.2	13.9	8	4.9	8.4
9	10.8	13.8	9	5.5	8.5
10	11.0	15.2	10	5.8	10.0
11	12.0	15.4	11	5.2	8.3
12	11.7	16.8	12	5.0	7.9
13	11.6	16.7	13	3.8	6.1
14	11.9	14.6	14	5.4	9.2
15	10.6	14.3	15	3.8	5.4
16	10.4	14.9	16		

Batavus Flipped

	Slalom			Slow	
	mean	max		mean	max
1	10.6	14.0	1	7.2	8.8
2	10.3	16.2	2	5.7	7.1
3	10.9	13.9	3	5.4	8.4
4	10.0	17.2	4	4.1	6.9
5	12.9	18.2	5	5.6	7.7
6	11.0	15.2	6	4.8	7.3
7	10.7	17.7	7	4.6	6.9
8	11.0	14.3	8	5.7	6.9
9	10.9	17.5	9	4.4	7.9
10	11.1	14.3	10	6.0	9.6
11	11.2	16.2	11	5.0	7.5
12	10.0	15.1	12	5.5	8.1
13	11.2	17.3	13	5.3	7.6
14	11.5	16.1	14	5.8	7.3
15	11.4	16.0	15	6.0	7.9
16			16	5.7	6.9

Gazelle

	Slalom			Slow	
	mean	max		mean	max
1	11.1	14.8	1	5.2	7.1
2	10.7	16.0	2	4.8	6.4
3	11.0	14.3	3	5.6	6.3
4	11.3	14.5	4	5.2	7.0
5	-	-	5	4.9	6.9
6	10.9	16.1	6	5.0	7.4
7	10.4	14.9	7	4.4	7.8
8	10.9	17.2	8	4.2	9.2
9	10.9	14.6	9	4.9	8.9
10	11.2	15.9	10	5.0	6.1
11			11	5.2	6.6
12			12	5.0	6.5
13			13	6.0	9.2
14			14		
15			15		
16			16		

Test Trike 1 - piet

	Slalom			Slow	
	mean	max		mean	max
1	7.2	14.0	1	4.5	7.0
2	10.1	14.6	2	3.7	6.9
3	11.1	15.0	3	3.9	7.3
4	8.8	14.0	4	5.0	8.5
5	11.2	15.2	5	3.6	6.3
6	12.1	15.5	6	5.2	8.2
7	10.9	15.7	7	4.5	8.1
8	11.7	15.0	8	3.8	6.3
9	10.8	14.5	9	4.5	6.2
10	10.3	14.9	10	3.8	5.6
11	11.9	14.6	11	3.6	7.9
12			12	3.9	6.8
13			13		
14			14		
15			15		
16			16		

Test Trike 2 - piet

	Slalom			Slow	
	mean	max		mean	max
1	9.8	14.3	1	5.0	8.5
2	10.5	13.9	2	-	-
3	11.3	15.8	3	3.6	6.3
4	11.7	14.3	4	5.1	8.0
5	10.9	13.9	5	4.5	7.6
6	11.1	13.4	6	4.7	6.2
7	-	-	7	4.1	7.3
8	10.9	12.9	8	4.5	6.8
9	10.3	14.2	9		
10	11.0	15.0	10		
11			11		
12			12		
13			13		
14			14		
15			15		
16			16		

Giant

	Slalom			Slow	
	mean	max		mean	max
1	11.2	14.0	1	5.1	7.9
2	10.9	13.9	2	4.0	5.9
3		11 14.8	3	5.3	8.0
4	11.3	14.2	4	3.8	5.6
5	12.0	17.6	5	4.4	6.5
6	11.0	15.0	6	4.3	7.1
7	10.9	13.8	7	5.8	6.8
8	11.8	14.6	8	4.3	6.2
9			9	4.7	6.8
10			10		
11			11		
12			12		
13			13		
14			14		
15			15		
16			16		

TT1

	Slalom			Slow	
	mean	max		mean	max
1	8.8	11.9	1	4.8	7.0
2	8.9	13.2	2	4.4	6.9
3	8.9	13.3	3	4.5	7.3
4	9.3	13.0	4	4.1	5.8
5	6.4	12.4	5	4.3	6.4
6	9.4	12.1	6	4.0	5.6
7	9.4	12.4	7	4.0	6.7
8	8.4	14.4	8	4.5	6.7
9	7.9	12.9	9	4.0	5.6
10	9.7	13.2	10	3.8	5.8
11	9.7	14.2	11	3.9	6.3
12	9.8	12.0	12	4.0	7.5
13	10.6	14.0	13	5.0	7.3
14	10.7	14.0	14	4.4	5.8
15	8.9	12.3	15	4.3	6.7
16	8.7	12.7			
17	11.6	13.0			
18	11.5	12.6			

TT2

	Slalom			Slow	
	mean	max		mean	max
1	11.3	14.3	1	5.1	9.4
2	9.5	13.5	2	4.8	7.6
3	10.7	13.3	3	5.5	7.1
4	11.1	15.6	4	5.6	7.8
5	9.8	12.7	5	5.9	8.6
6	9.4	14.0	6	5.2	7.9
7	10.8	14.2	7	4.8	6.8
8	9.0	12.5	8	4.7	6.9
9	9.9	12.6	9	3.7	6.2
10	9.3	13.4	10	8.6	18.6
11	9.7	13.1	11	6.0	10.4
12	9.1	13.2	12	3.8	6.9
13	11.5	14.6	13	5.7	6.3
14	9.6	13.3	14	5.5	7.8
15	11.8	13.6	15	5.4	6.8
16					
17					
18					

TT3

	Slalom			Slow	
	mean	max		mean	max
1	9.3	11.9	1	4.8	7.6
2	10.7	12.8	2	5.4	6.9
3	9.8	13.1	3	5.3	7.4
4	10.7	13.6	4	4.8	7.4
5	9.6	11.7	5	5.6	8.3
6	9.6	12.3	6	5.3	7.4
7	8.8	11.6	7	5.0	8.5
8	10.0	12.0	8	5.9	7.8
9	9.0	11.8	9	5.2	6.9
10	10.4	12.6	10	5.1	7.3
11	9.9	12.2	11	5.2	8.4
12	9.6	12.7	12	5.2	7.5
13	10.2	12.6	13	5.3	7.3
14	9.2	12.2	14	5.2	7.8
15	8.3	11.9	15	4.6	8.1
16					
17					
18					

TT4

	Slalom			Slow	
	mean	max		mean	max
1	7.3	9.9	1	5.4	6.3
2	6.9	11.2	2	5.2	7.3
3	7.2	9.5	3	5.6	8.4
4	7.1	11.7	4	4.9	7.5
5	6.5	11.6	5	5.4	6.9
6	8.9	13.6	6	5.0	7.2
7	8.1	11.9	7	4.6	6.6
8	6.0	9.1	8		
9			9		
10			10		
11			11		
12			12		
13			13		
14			14		
15			15		
16					
17					
18					

Figure C.2: Velocity data for all valid trials.